


Xenogeneic and Allogeneic Mesenchymal Stem Cells Effectively Protect the Lung Against Ischemia-reperfusion Injury Through Downregulating the Inflammatory, Oxidative Stress, and Autophagic Signaling Pathways in Rat

Kun-Chen Lin¹, Jun-Ning Yeh², Yi-Ling Chen^{3,4,5},
John Y. Chiang^{6,7}, Pei-Hsun Sung^{3,5}, Fan-Yen Lee^{4,5,8,9},
Jun Guo^{2,*}, and Hon-Kan Yip^{3,4,5,10,11,12,*} 

Cell Transplantation
Volume 29: 1–20
© The Author(s) 2020
Article reuse guidelines:
sagepub.com/journals-permissions
DOI: 10.1177/0963689720954140
journals.sagepub.com/home/ccl


Abstract

This study tested the hypothesis that both allogeneic adipose-derived mesenchymal stem cells (ADMSCs) and human inducible pluripotent stem cell-derived MSCs (iPS-MSCs) offered a comparable effect for protecting the lung against ischemia-reperfusion (IR) injury in rodent through downregulating the inflammatory, oxidative stress, and autophagic signaling pathways. Adult male Sprague–Dawley rats ($n = 32$) were categorized into group 1 (sham-operated control), group 2 (IRI), group 3 [IRI + ADMSCs (1.0×10^6 cells)/tail-vein administration at 0.5/18/36 h after IR], and group 4 [IRI + iPS-MSCs (1.0×10^6 cells)/tail-vein administration at 0.5/18/36 h after IR], and lungs were harvested at 72 h after IR procedure. *In vitro* study demonstrated that protein expressions of three signaling pathways in inflammation (TLR4/MyD88/TAK1/IKK/I- κ B/NF- κ B/Cox-2/TNF- α /IL-1 β), mitochondrial damage/cell apoptosis (cytochrome C/cyclophilin D/DRP1/ASK1/APAF-1/mitochondrial-Bax/caspase3/8/9), and autophagy/cell death (ULK1/beclin-1/Atg5,7,12, ratio of LC3B-II/LC3B-I, p-AKT/m-TOR) were significantly higher in lung epithelial cells + 6h hypoxia as compared with the control, and those were significantly reversed by iPS-MSC

¹ Department of Anesthesiology, Kaohsiung Chang Gung Memorial Hospital and Chang Gung University College of Medicine, Kaohsiung

² Department of Cardiology, The First Affiliated Hospital, Jinan University, Guangzhou, China

³ Division of Cardiology, Department of Internal Medicine, Kaohsiung Chang Gung Memorial Hospital and Chang Gung University College of Medicine, Kaohsiung

⁴ Institute for Translational Research in Biomedicine, Kaohsiung Chang Gung Memorial Hospital, Kaohsiung

⁵ Center for Shockwave Medicine and Tissue Engineering, Kaohsiung Chang Gung Memorial Hospital, Kaohsiung

⁶ Department of Computer Science and Engineering, National Sun Yat-Sen University, Kaohsiung

⁷ Department of Healthcare Administration and Medical Informatics, Kaohsiung Medical University, Kaohsiung

⁸ Division of Thoracic and Cardiovascular Surgery, Department of Surgery, Kaohsiung Chang Gung Memorial Hospital and Chang Gung University College of Medicine, Kaohsiung

⁹ Division of Cardiovascular Surgery, Department of Surgery, Tri-Service General Hospital, National Defense Medical Center, Taipei

¹⁰ Department of Medical Research, China Medical University Hospital, China Medical University, Taichung

¹¹ Department of Nursing, Asia University, Taichung

¹² Division of Cardiology, Department of Internal Medicine, Xiamen Chang Gung Hospital, Xiamen, Fujian, China

*Both the authors contributed equally to this article

Submitted: May 21, 2020. Revised: August 4, 2020. Accepted: August 7, 2020.

Corresponding Authors:

Jun Guo, Department of Cardiology, The First Affiliated Hospital, Jinan University, Guangzhou 510630, China.

Email: dr.guojun@163.com;

Hon-Kan Yip, Kaohsiung Chang Gung Memorial Hospital, 123 Dapi Rd., Niasung Dist., Kaohsiung.

Email: han.gung@msa.hinet.net.



Creative Commons Non Commercial CC BY-NC: This article is distributed under the terms of the Creative Commons Attribution-NonCommercial 4.0 License (<https://creativecommons.org/licenses/by-nc/4.0/>) which permits non-commercial use, reproduction and distribution of the work without further permission provided the original work is attributed as specified on the SAGE and Open Access pages (<https://us.sagepub.com/en-us/nam/open-access-at-sage>).

treatment (all $P < 0.001$). Flow cytometric analysis revealed that percentages of the inflammatory cells in bronchioalveolar lavage fluid and circulation, and immune cells in circulation/spleen as well as circulatory early and late apoptotic cells were highest in group 2, lowest in group 1, and significantly higher in group 3 than in group 4 (all $P < 0.0001$). Microscopy showed the lung injury score and numbers of inflammatory cells and Western blot analysis showed the signaling pathways of inflammation, mitochondrial damage/cell apoptosis, autophagy, and oxidative stress exhibited an identical pattern of flow cytometric results among the four groups (all $P < 0.0001$). Both xenogeneic and allogenic MSCs protected the lung against IRI via suppressing the inflammatory, oxidative stress, and autophagic signaling.

Keywords

xenogeneic and allogenic MSCs, acute lung ischemia-reperfusion injury, inflammation, oxidative stress, apoptosis, autophagy

Introduction

Physiologically, the lung is an extremely crucial vital organ due to its unique function in providing direct gaseous exchange with the environment through the abundant alveolar surface area and delicate alveolar capillary network with great intrinsic elasticity and good compliance. As such, it is vulnerable to acute lung injury (ALI)/acute ischemia-reperfusion injury (IRI) in those detrimental conditions such as lung transplantation, cardiopulmonary bypass, resuscitation for circulatory arrest, hypoxic respiratory failure, smoke or toxic chemical inhalation, viral infection, and sepsis, highlighting that ALI/acute lung IRI resulted from diverse disease entities^{1–8}. Basic researches have clearly shown that inflammatory cells act as the coordinators for ischemia-reperfusion (IR)-elicited pulmonary injury in response to inflammatory response and oxidative stress^{9–11}. Additionally, the productions of reactive oxygen species, proinflammatory cytokines, and adhesion molecules have also been identified to be consequential contributors to the lung injury in situation of IRI^{10,12–16}. Furthermore, damage-associated molecular patterns (DAMPs)-inflammatory axis and autophagic signaling play a crucial role on ischemia/inflammatory-related organ damage^{17–22}, suggesting that these signaling pathways surely involve in the ALI/IRI. Surprisingly, despite state-of-the-art advance in pharmacological therapy, technical improvement, aggressive intervention, guideline renewal, and education, ALI/IRI still lead to a universally unacceptable high in-hospital morbidity and mortality^{23–25}. Accordingly, to develop a new therapeutic modality is utmost important and urgent for physicians and patients.

Abundant data have shown that mesenchymal stem cells (MSCs), especially those of adipose-derived mesenchymal stem cells (ADMSCs), have properties of anti-inflammation and immunomodulation^{24,26–31}. Accordingly, ADMSC therapy is effective and promising on protecting the organs from ischemia or IRI, which in turn, preserves organ function^{24,26–31}. On the other hand, it is well recognized that induced pluripotent stem cells (iPSCs) are reprogrammed cells that have features similar to embryonic stem cells, such as the capacity of self-renewal and differentiation into various types of cell lineage. Interestingly, growing data have revealed that human inducible pluripotent stem cell-

derived MSCs (iPS-MSCs) also has capacity of tissue regeneration and protect the organ from ischemia/IRI^{32–38}. However, the therapeutic effect of iPS-MSCs on acute lung IRI remains uncertain. Furthermore, whether ADMSCs is superior to iPS-MSCs or vice versa in terms of therapeutic effects has not yet been studied. Moreover, the underlying mechanism involved in protecting the lung from acute IRI after these two stem cell therapy has not been clarified, especially the data are much more limited in the case of iPS-MSCs therapy. This study was, therefore, designed to answer these unresolved questions.

Materials and Methods

Ethics Statement

All animal procedures were approved by the Institute of Animal Care and Use Committee at Kaohsiung Chang Gung Memorial Hospital (Affidavit of Approval of Animal Use Protocol No. 2018032103) and performed in accordance with the Guide for the Care and Use of Laboratory Animals. Animals were housed in an Association for Assessment and Accreditation of Laboratory Animal Care International (AAALAC; Frederick, MD, USA)-approved animal facility in our hospital with controlled temperature and light cycles (24°C and 12/12 light cycle).

Animal Model of Acute Lung IRI and Animal Grouping

Pathogen-free, adult male Sprague–Dawley (SD) rats ($n = 32$) weighing 320–350 g (BioLASCO Taiwan Co., Ltd. Taipei, Taiwan) were utilized in the present study. The procedure and protocol have been described in our previous reports^{39,40}. In detail, all animals were anesthetized by chloral hydrate (35 mg/kg i.p.) plus inhalational isoflurane (2.0%) and placed in a supine position on a warming pad at 37°C, followed by endotracheal intubation with positive-pressure ventilation (180 ml/min) with room air using a Small Animal Ventilator (SAR-830/A, CWE, Inc., USA). Under sterile conditions, the lung was exposed via a left thoracotomy. Lung IR was then conducted in designated (i.e., groups 2 to 4) animals on which a left thoracotomy was performed with the left main bronchus and blood supplies to the left lung totally clamped for 30 min using nontraumatic

vascular clips before reperfusion for 72 h. Successful clamping was confirmed by the observation of a lack of inflation of the left lung on mechanical ventilation. Sham-operated rats subjected to left thoracotomy only served as normal controls.

The CellTracker™ Orange CMRA cell-labeling solution (Molecular Probes, Inc. Eugene, OR, USA) (25 μ M) was added to the culture medium 37°C, 30 min prior to IR procedure for ADMSC and iPS-MSC labeling. After completion of cells labeling, intravenous infusion of allogenic ADMSCs or xenogeneic iPS-MSCs was performed at 30 min, 18 h, and 36 h after IR procedure in groups 3 or 4, respectively. The dosage of ADMSCs utilized in this procedure was based on our recent reports with minimal modification^{26–28}.

The adult male SD rats ($n = 32$) were equally categorized into four groups, i.e., group 1 [sham-operated control (SC)], group 2 (IRI + normal saline/3.0 cm³ via i.p. injection), group 3 [IRI+ allogenic ADMSC (1.2×10^6 cells) from tail-vein administration at 30 min, 18 h, and 36 h after IR procedure], and group 4 [IRI + human-derived iPS-MSC (1.2×10^6 cells) from tail-vein administration at 30 min, 18 h, and 36 h after IR procedure], respectively.

In Vitro Study for Determining the Autophagic and DAMPs-inflammatory Signaling Pathways

L2 cells (i.e., rat lung epithelial cell line) purchased from Bioresource Collection and Research Center, Taiwan were utilized in the present study. Under the hypoxia and reperfusion condition (i.e., 1% oxygen for 6 h then return to room temperature for 24 h, i.e., mimicked IR injury), L2 cells were cultured (5.0×10^5 cells) in Transwell (bottom) with and without iPS-MSC (1.0×10^5) (at the top of the bottle) for 24 h, and then the cells were collected and Western blot analysis was performed for protein expressions of autophagic and DAMPs-inflammatory biomarkers.

Allogeneous ADMSC Preparation and Culturing

Adipose tissue surrounding the epididymis was carefully dissected, excised, and prepared from additional six animals based on our previous reports^{39,40}. After isolation, adipose tissue was cut into <1 mm³ pieces using a pair of sharp, sterile surgical scissors. Sterile saline (37°C) was added to the homogenized adipose tissue in a ratio of 3:1 (saline:adipose tissue), followed by the addition of stock collagenase solution to a final concentration of 0.5 units/ml. The centrifuge tubes with the contents were placed and secured on a Thermaline shaker and incubated with constant agitation for 60 ± 15 min at 37°C. After 40 min of incubation, the content was triturated with a 25 ml pipette for 2–3 min. The cells obtained were placed back to the rocker for incubation. The contents of the flask were transferred to 50 ml tubes after digestion, followed by centrifugation at 600 \times g for 5 min at room temperature. The cell pellets thus obtained were resuspended in 40 ml saline and then centrifuged again at 600 \times g for 5 min at room temperature. After being resuspended

again in 5 ml saline, the cell suspension was filtered through a 100 μ m filter into a 50 ml conical tube to which 2 ml of saline was added to rinse the remaining cells through the filter. The tubes were centrifuged for a third time at 600 \times g for 5 min at room temperature. The cells were resuspended in saline. An aliquot of cell suspension will be then removed for cell culture in Dulbecco's modified Eagle's medium (DMEM)-low glucose medium (Gibco, Carlsbad, CA, USA). containing 10% fetal bovine serum for 14 days. Approximately 5.5×10^6 ADMSCs were obtained from each rat.

In Vitro Study of Cell Culturing for Differentiation of Human iPSC into MSCs

The procedure and protocol of human iPSC culture for differentiation into MSCs were based on the manufacturer's instruction and our recent report⁴¹. In detail, by day 1, human iPSCs (mTeSR™1; StemCell, #28315) were first washed by 5 ml phosphate buffered saline (PBS), followed by 2 ml Accutase (Gibco, #A1110501; Accutase:PBS = 1:1) and allowed the reaction in incubator for 1 min. The 2 ml KO DMEM/F12 (Gibco, #12660012) was added and the cells were then collected in 15 ml centrifugation tube and centrifuged (200 \times g) for 5 min. The cells were then cultured in 10 cm dish for 24 h in mTeSR™1 culture medium.

By day 2, the cells (mTeSR™1) were collected and washed by 5 ml PBS, followed by adding STEMdiff™-ACF Mesenchymal Induction Medium (StemCell, #05241) and then cultured in incubator for 24 h. The STEMdiff™-ACF Mesenchymal Induction Medium was refreshed once/day from days 1 to 3. This procedure was repeated at days 3 to 6. From days 7 to 21, the procedure was repeated daily with culture medium regularly refreshed for every 3 days.

Histological Assessment of Lung Injury Score and Crowded Score of Lung Parenchyma by Day 3 After IR Procedure

For identification of number of alveolar sac distributed n in lung parenchyma, left lung specimens from every animal were fixed in 4% paraformaldehyde prior to embedding in paraffin and the lung tissue was sectioned at 5 μ m for light microscopic analysis. The hematoxylin and eosin (H&E) stain was performed for the assessment of number of alveolar sacs based on our previous reports in a blind fashion^{39,40}. Three lung sections from each rat were analyzed with three randomly selected high-power fields (HPFs, i.e., 100 \times) in each section. The mean number per HPF for each animal was then determined by summation of all numbers divided by 9. The extent of crowded area, defined as region of thickened septa in lung parenchyma associated with partial or complete collapse of alveoli on H&E-stained sections, was performed in a blind fashion. The scoring system adopted was as follows: 0 = no detectable crowded area, 1 = <15% of crowded area, 2 = 15%–25% of crowded area, 3 = 26%–50% of

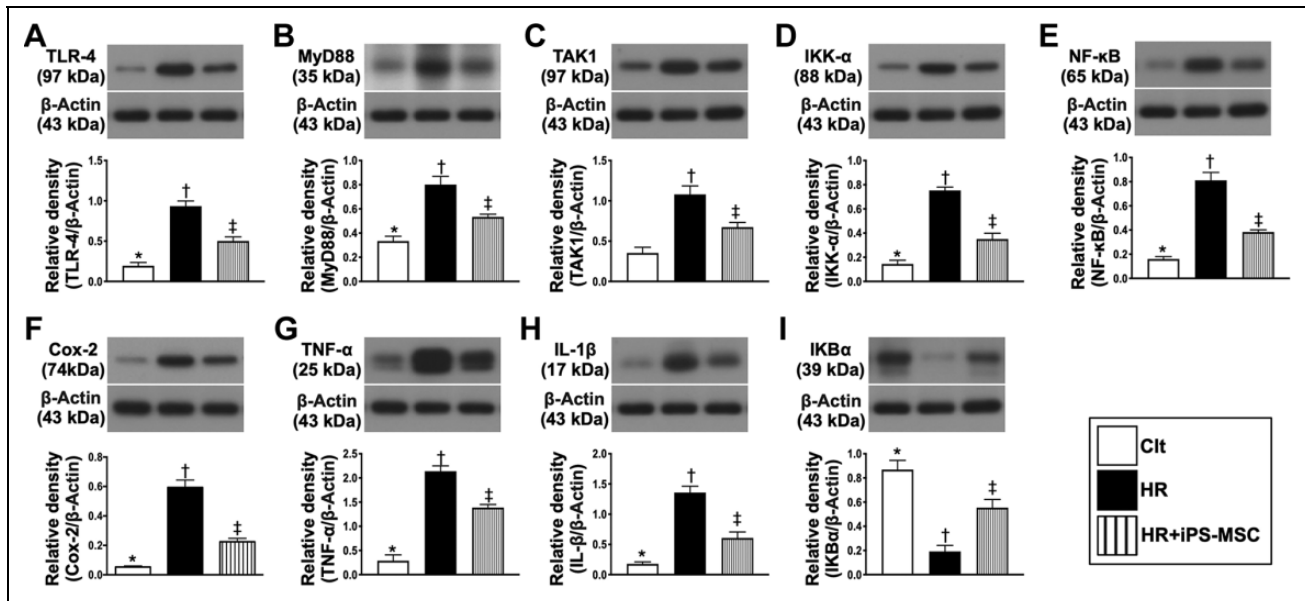


Fig. 1. iPS-MSCs effectively suppressed the inflammatory signaling pathway. (A to I) Protein expressions of TLR-4 (A), MyD88 (B), TAK1 (C), IKK- α (D), NF- κ B (E), Cox-2 (F), TNF- α (G), IL- β (H), and nuclear factor of kappa light polypeptide gene enhancer in B-cells inhibitor alpha (IKB α) (I), respectively, * versus other groups with different symbols (†, ‡), $P < 0.001$. All statistical analyses were performed by one-way ANOVA, followed by Bonferroni multiple comparison post hoc test ($n = 3$ for each group). Symbols (*, †, ‡) indicate significance (at 0.05 level). ANOVA: analysis of variance; Clt: control; HR: hypoxia-reperfusion; IKK- α : inhibitory- κ B kinase α ; IL: interleukin; iPS-MSCs: human inducible pluripotent stem cell-derived mesenchymal stem cells; MyD88: myeloid differentiation primary response 88; NF: nuclear factor; TAK1: transforming growth factor- β -activated kinase 1; TLR: toll-like receptor; TNF: tumor necrosis factor.

crowded area, 4 = 51%–75% of crowded area, and 5 = >75% of crowded area/HPF (100 \times).

Flow Cytometric Quantification of Immune and Inflammatory Cells in Circulation, Spleen, and Bronchioalveolar Lavage

The procedure and protocol of flow cytometry for identification and quantification of inflammatory and immune cells were based on our previous report⁴². Briefly, prior to sacrificing the animals, peripheral blood mononuclear cells (PBMCs) were obtained from the tail vein using a 27# needle. PBMCs (1.0×10^6 cells) were triple stained with FITC-anti-CD3 (BioLegend, San Diego, CA, USA), PE-anti-CD8a (BD Biosciences, San Jose, CA, USA), and PE-CyTM5 anti-CD4 (BD Biosciences). To identify CD4⁺CD25⁺Foxp3⁺ regulatory T cells (Tregs), PBMCs were triple stained with Alexa Fluor[®] 488-anti-CD25 (BioLegend), PE-anti-Foxp3 (BioLegend), and PE-CyTM5 anti-CD4 (BD Biosciences) according to the manufacturer's protocol of Foxp3 Fix/Perm buffer set. The numbers of CD3⁺CD4⁺ helper T cells, CD3⁺CD8⁺ cytotoxic T cells, and CD4⁺CD25⁺Foxp3⁺ Tregs were analyzed using flow cytometry (FC500, Beckman Coulter, Brea, CA, USA). Additionally, the numbers of inflammatory cells (CD11b⁺/CD86⁺, CD11b⁺/CD206⁺, CD68⁺/CD80⁺, CD68⁺/CD163⁺, CD11b⁺/c⁺, Ly6G⁺)

in circulation or in bronchioalveolar lavage (BAL) fluid were also assessed by flow cytometry.

A Pilot Study for Comparison of the Therapeutic Effect Between iPS-MSCs and ADMSCs on Attenuating the Albumin Leakage into the Bronchioalveolar Space at 72 h After Acute Lung IR Procedure

To elucidate whether the iPS-MSCs was superior to ADMSCs or vice versa on protecting the lung against acute IRI in rat, a pilot study was done among the aforementioned four groups of 16 additional animals (i.e., $n = 4$ in each group). The results of the BAL fluid showed that the concentration of leaked albumin was lowest in group 1, highest in group 2, and significantly lower in group 4 as compared with that of group 3, implicating that iPS-MSCs offered a better protective effect on lung after acute lung IRI. Accordingly, the iPS-MSCs were utilized for the *in vitro* study (Supplemental Fig. 1).

Flow Cytometric Analysis for Assessment of Cellular Apoptosis

The percentages of viable and apoptotic cells were determined by flow cytometry using double staining of annexin V and propidium iodide (PI). This is a simple and popular method for the identification of apoptotic cells [i.e., early

(annexin V+/PI-) and late (annexin V+/PI+) phases of apoptosis].

Western Blot Analysis of Lung Specimen

The procedure and protocol for Western blot have been reported in our previous studies^{39,40}. In detail, equal amounts (50 µg) of protein extracts will be loaded and separated by sodium dodecyl sulfate polyacrylamide gel electrophoresis using acrylamide gradients. After electrophoresis, the separated proteins were transferred electrophoretically to a polyvinylidene difluoride membrane (Amersham Biosciences, Amersham, UK). Nonspecific sites will be blocked by incubation of the membrane in blocking buffer [5% nonfat dry milk in T-TBS (TBS containing 0.05% Tween 20)] overnight. The membranes will be incubated with the indicated primary antibodies [toll-like receptor (TLR)-4 (1:500, Abcam, Cambridge, UK), myeloid differentiation primary response 88 (MyD88) (1:2,000, Abcam), transforming growth factor-β-activated kinase 1 (TAK1) (1:1,000, Cell Signaling, Danvers, MA, USA), IκB kinase (IKK)-α (1:5,000, Abcam), nuclear factor (NF)-κB (1:600, Abcam), Cox-2 (1:1,000, Abcam), tumor necrosis factor (TNF)-α (1:1,000, Cell Signaling), interleukin (IL)-1β (1:1,000, Cell Signaling), IκBα (1:1,000, Cell Signaling), cytosolic cytochrome C (1:1,000, BD Biosciences), mitochondrial cytochrome C (1:1,000, BD Biosciences), Cyclophilin D (CyPD) (1:3,000, Abcam), dynamin-related protein (DRP) 1 (1:1,000, Cell Signaling), apoptosis signal-regulating kinase 1 (ASK1) (1:1,000, Abcam), apoptotic protease activating factor 1 (1:1,000, Cell Signaling), mitochondrial Bax (1:1,000, Abcam), cleaved caspase 3 (1:1,000, Cell Signaling), caspase 8 (1:1,000, Cell Signaling), caspase 9 (1:1,000, Cell Signaling), Bcl-2 (1:1,000, Arigobio), Bcl-XL (1:1,000, Abcam), unc-51 like autophagy activating kinase 1 (ULK1) (1:1,000, Cell Signaling), beclin-1 (1:1,000, Cell Signaling), Atg5 (1:1,000, Cell Signaling), Atg7 (1:1,000, Cell Signaling), Atg12 (1:1,000, Cell Signaling), LC3B-I (1:2,000, Abcam), LC3B-II (1:2,000, Abcam), phosphorylated (p)-Akt (1:1,000, Cell Signaling), p-m-TOR (1:1,000, Cell Signaling), gp91phox (1:750, Sigma), p22phox (1:1,000, Abcam), and actin (1:10,000, Chemicon)] for 1 h at room temperature. Horseradish peroxidase-conjugated anti-rabbit immunoglobulin IgG (1:2,000, Cell Signaling) was used as a secondary antibody for 1-h incubation at room temperature. The washing procedure was repeated eight times within 1 h. Immunoreactive bands were visualized by enhanced chemiluminescence (ECL; Amersham Biosciences) and exposed to Biomax L film (Kodak, Rochester, NY, USA). For purposes of quantification, ECL signals were digitized using Labwork software (UVP, Waltham, MA, USA).

Immunofluorescent Study

The procedure and protocol for immunofluorescent (IF) staining have been reported in our previous studies^{39,40}. For

IF staining, rehydrated paraffin sections were first treated with 3% H₂O₂ for 30 min and incubated with Immuno-Block reagent (BioSB, Santa Barbara, CA, USA) for 30 min at room temperature. Sections were then incubated with primary antibodies specifically against γ-H2AX (1:500, Abcam), F4/80 (1:100, Santa Cruz Biotechnology, Dallas, TX, USA), and CD14 (1:200, Bioss, Woburn, MA, USA) at 4°C overnight. Alexa Fluor488, Alexa Fluor568, or Alexa Fluor594-conjugated goat anti-mouse or rabbit IgG were used to localize signals. Sections were finally counterstained with 4',6-diamidino-2-phenylindole and observed with a fluorescence microscope equipped with epifluorescence (Olympus IX-40).

Three lung sections were analyzed for each rat. For quantification, three randomly selected HPFs (×400 for IF study) were analyzed in each section. The mean number of positively stained cells per HPF for each animal was then determined by summation of all numbers divided by 9.

Statistical Analysis

Quantitative data will be expressed as mean ± standard deviation. Statistical analysis was adequately performed by analysis of variance followed by Bonferroni multiple comparison post hoc test. Statistical analysis was performed using SPSS statistical software for Windows version 13 (SPSS for Windows, version 13; SPSS, Chicago, IL, USA). A *P*-value of less than 0.05 will be considered statistically significant.

Results

iPS-MSCs Effectively Suppressed the Activations of Inflammatory, Mitochondrial-damaged/Cell Death, and Autophagic Signaling Pathways

While the role of ADMSC on anti-inflammation and immunomodulation has been well recognized by our previous basic researches^{26–28,39,40,43}, the role of iPS-MSCs on regulating the inflammatory signaling remains yet to be fully investigated (Figs. 1–5). To verify whether iPS-MSCs share the capacity of ADMSC on inhibiting the up-/down-stream inflammatory signaling pathways, the L2 cells were cultured in Transwell undergoing the hypoxia and reperfusion (H-R) condition (i.e., for mimicked IR condition) (refer Materials and Methods for detailed information). The results demonstrated that the protein expressions of TLR4, MyD88, TAK1, IKK-α, NF-κB, Cox-2, TNF-α, and IL-1β, the indices of up-/down-stream inflammatory signaling pathways, were significantly upregulated in L2 cells + H-R (group 2) as compared with control group (group 1), and those were significantly downregulated in H-R condition treated by iPS-MSCs (group 3) (Fig. 1). On the other hand, the protein expression of p-IKBα, a protein for transmitting the signaling from upper to the lower

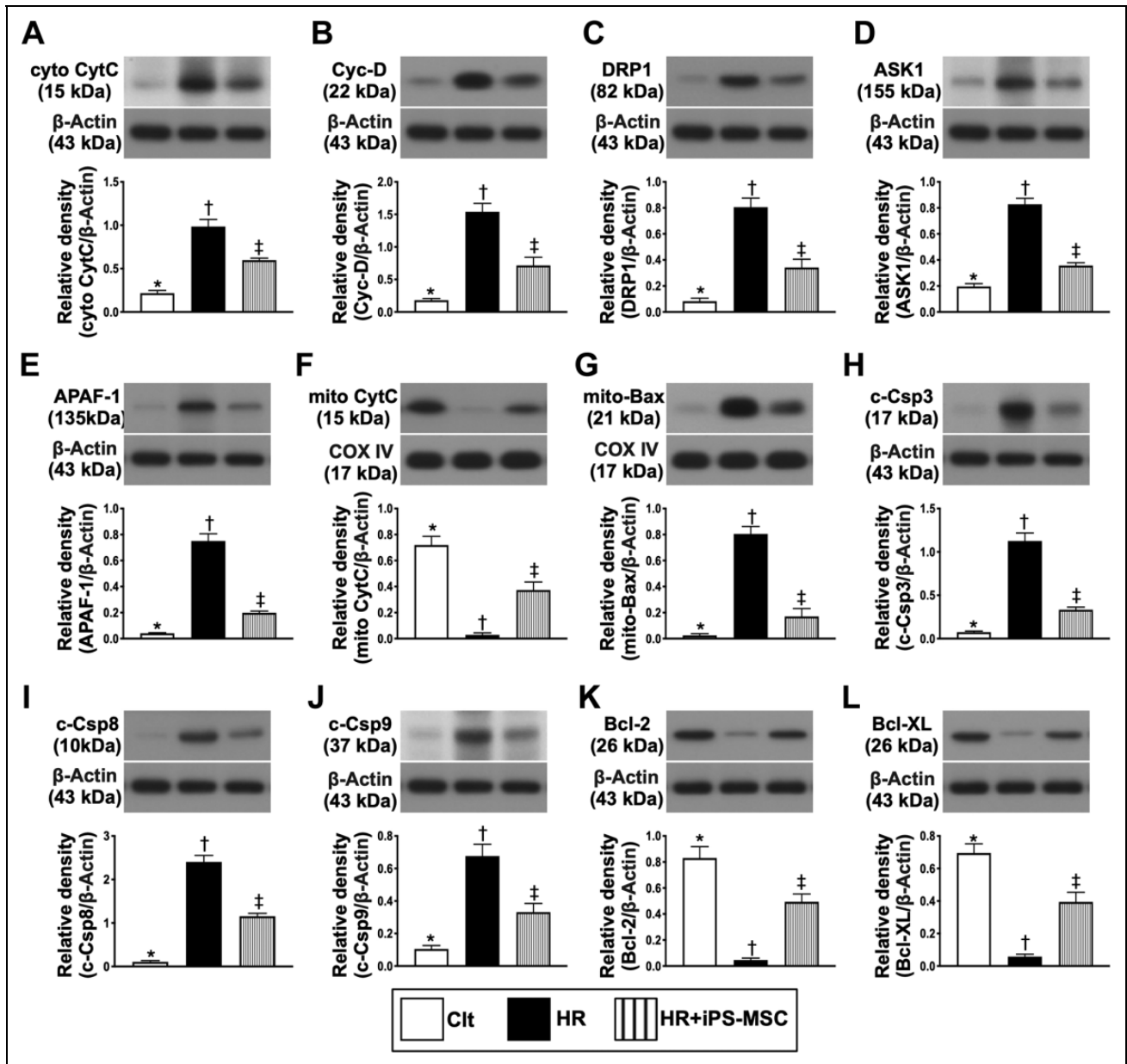


Fig. 2. iPS-MSCs effectively suppressed the mitochondrial damage and cell apoptotic signaling pathways. (A to E) Protein expressions of cyto-CytC (A), cyc-D (B), DRP1 (C), ASK1 (D), APAF-1 (E), and mito-CytC (F), respectively, * versus other groups with different symbols (\dagger , \ddagger), $P < 0.001$. (G to L) Protein expressions of mitochondrial (mito)-Bax (G), c-Csp3 (H), c-Csp8 (I), c-Csp9 (J), Bcl-2 (K), and Bcl-XL (L), respectively, * versus other groups with different symbols (\dagger , \ddagger), $P < 0.001$. All statistical analyses were performed by one-way ANOVA, followed by Bonferroni multiple comparison post hoc test ($n = 3$ for each group). Symbols (*, \dagger , \ddagger) indicate significance (at 0.05 level). ANOVA: analysis of variance; APAF-1: apoptotic protease activating factor 1; ASK1: apoptosis signal-regulating kinase 1; c-Csp3: cleaved caspase 3; Clt: control; cyc-D: cyclophilin D; cyto-CytC: cytosolic cytochrome C; DRP1: dynamin-related protein 1; HR: hypoxia-reperfusion; iPS-MSCs: human inducible pluripotent stem cell-derived mesenchymal stem cells; mito-CytC: mitochondrial cytochrome C.

signaling pathway, displayed an opposite pattern of TLR4 among the three groups.

To further verify whether iPS-MSCs also has the ability on regulating the mitochondrial damage/cell apoptosis signaling, L2 cells were cultured as the condition depicted in Fig. 1. As we expected, the results showed that the protein expressions of cytosolic cytochrome C,

cyclophilin D, DRP1, ASK1 and APAF-1, five indicators of mitochondrial-damaged biomarkers, and protein expressions of mitochondrial Bax, caspases 3, 8 and 9, four indicators of cellular apoptosis, were significantly increased in group 2 than in group 1, and those were significantly reversed in group 3 (Fig. 2). On the other hand, protein expression of mitochondrial cytochrome C,

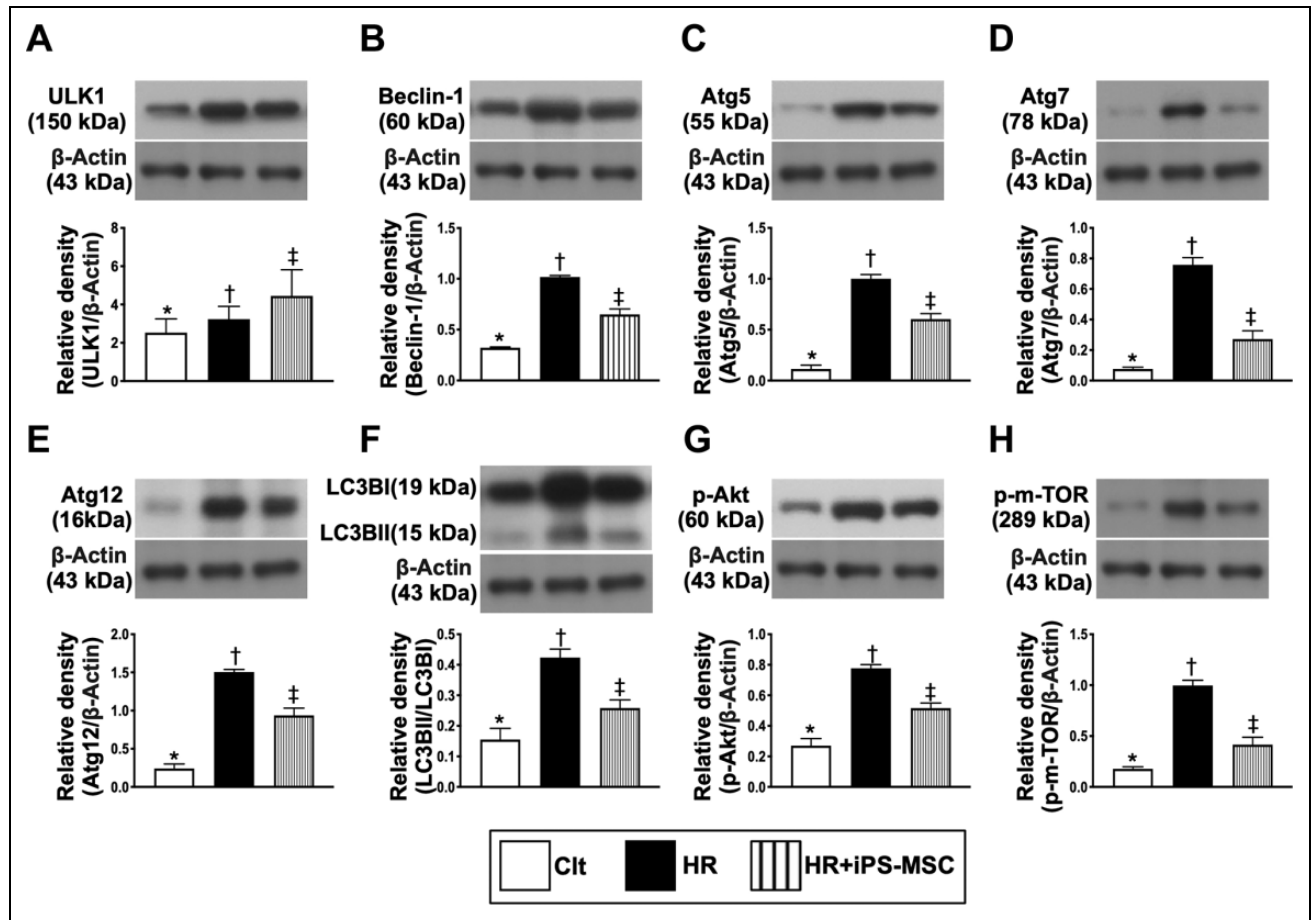


Fig. 3. iPS-MSCs effectively suppressed the autophagic and cell proliferation/death signaling pathways. (A to H) Protein expressions of autophagy activating kinase I (ULK1) (A), beclin-1 (B), Atg5 (C), Atg7 (D), Atg12 (E), ratio of LCB3-II/LC3B-I (F), phosphorylated (p)-Akt (G), and p-m-TOR (H), respectively, * versus other groups with different symbols (†, ‡), $P < 0.001$. All statistical analyses were performed by one-way ANOVA, followed by Bonferroni multiple comparison post hoc test ($n = 3$ for each group). Symbols (*, †, ‡) indicate significance (at 0.05 level). ANOVA: analysis of variance; Ctl: control; HR: hypoxia–reperfusion; iPS-MSCs: human inducible pluripotent stem cell-derived mesenchymal stem cells.

an indicator of mitochondrial integrity, and protein expression of Bcl-2 and Bcl-XL, two indices of antiapoptosis, displayed an opposite pattern of apoptosis among the three groups (Fig. 2).

Again, to further clarify the impact of iPS-MSCs on regulating the expression of the autophagic signaling, the L2 cells were once again cultured as the condition in Fig. 1. No doubt, the protein expressions of ULK1, beclin-1, Atg5, 7 and 12, ratio of LCB3-II/LC3B-I, six indices of autophagic biomarker, and protein expressions of p-AKT and m-TOR, two indicators of cell survival/cell death, were significantly higher in group 2 than in that of group 1, and those were significantly reversed in group 3 (Fig. 3). Based on the findings of Figs. 1–3, we proposed the underlying mechanism of xenogeneic MSCs protecting the lung epithelial cells from hypoxia–reperfusion injury in Figs. 4 and 5. Also, based on these findings, a lung IRI animal model was performed to further test hypothesis proposed.

Flow Cytometric Analyses of Inflammatory, Immune, and Apoptotic Cells by 72 h After Lung IR Procedure

To determine the change of bronchioalveolar and circulatory inflammatory cells, flow cytometric analysis was performed (Figs. 6 and 7). The result displayed that cellular expressions of CD11b+/CD86+, CD11b+/CD206+, and CD68+/CD80+ cells in BAL fluid, three indicators of acute inflammatory cells, were highest in group 2 (i.e., acute lung IR), lowest in group 1 (SC), and significantly higher in group 3 (acute lung IR + ADMSC) than in group 4 (acute lung IR + iPS-MSC) (Fig. 6). On the other hand, the number of CD68+/CD163+ cells in BAL fluid, an indicator of M2-like macrophages, was significantly and progressively increased from group 1 to group 4 (Fig. 6). Additionally, flow cytometric analysis identified that the circulatory inflammatory cells, including CD68+/CD80+, CD11b+, and Ly6G+ cells, were significantly higher in group 2 than

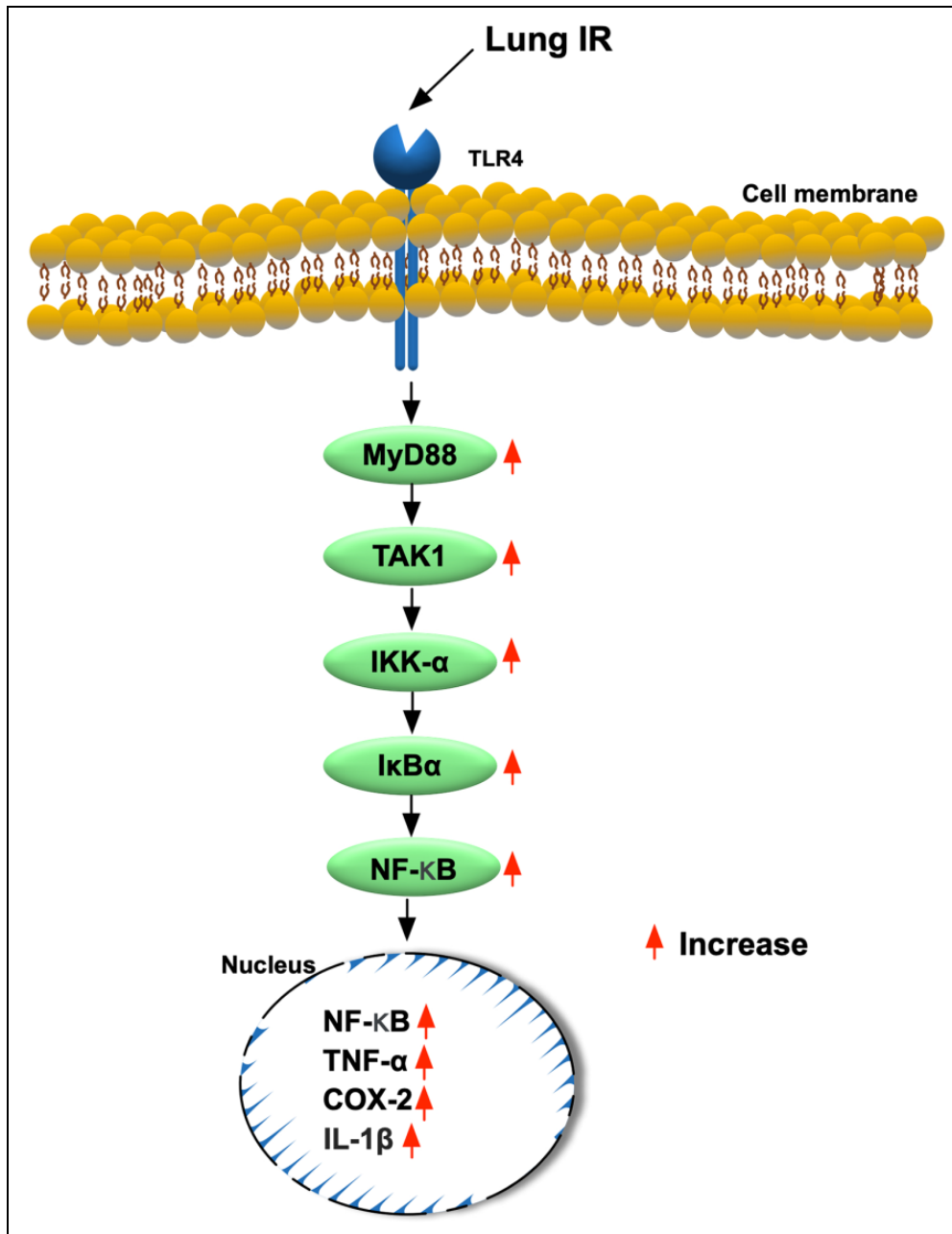


Fig. 4. Schematic proposed mechanism of inflammatory downstream signaling pathway in lung epithelial cells undergoing hypoxia–reperfusion stimulation. IR: ischemia-reperfusion.

in groups 1, 3, and 4, significantly higher in groups 3 and 4 than in group 1, and significantly higher in group 3 than in group 4 (Fig. 6). On the other hand, the number of CD68⁺/CD163⁺ cells in circulation was significantly and progressively increased from group 1 to group 4 (Fig. 6).

To clarify the alternations of immune cells in circulation and spleen, flow cytometric analysis was performed. The result showed that the cellular expressions of CD3⁺CD4⁺ helper T cells and CD3⁺CD8⁺ cytotoxic T cells in circulation and spleen displayed an identical pattern of circulatory inflammatory cells among the four groups. On the other

hand, the expression of CD4⁺CD25⁺Foxp3⁺ Tregs was progressively increased from groups 1 to 4, implying an intrinsic response to IR stimulation and further enhanced by MSC treatment (Fig. 7). Furthermore, numbers of the circulatory early and late apoptotic cells followed an identical pattern of inflammatory cells among the four groups (Fig. 7). Our findings suggested that the acute IR upregulated only local but systemic inflammatory-immune reactions which, in turn, participated in the damage of the lung organ after IR.

Consistently, the flow cytometric analysis exhibited that the early and late mononuclear cell apoptosis revealed an

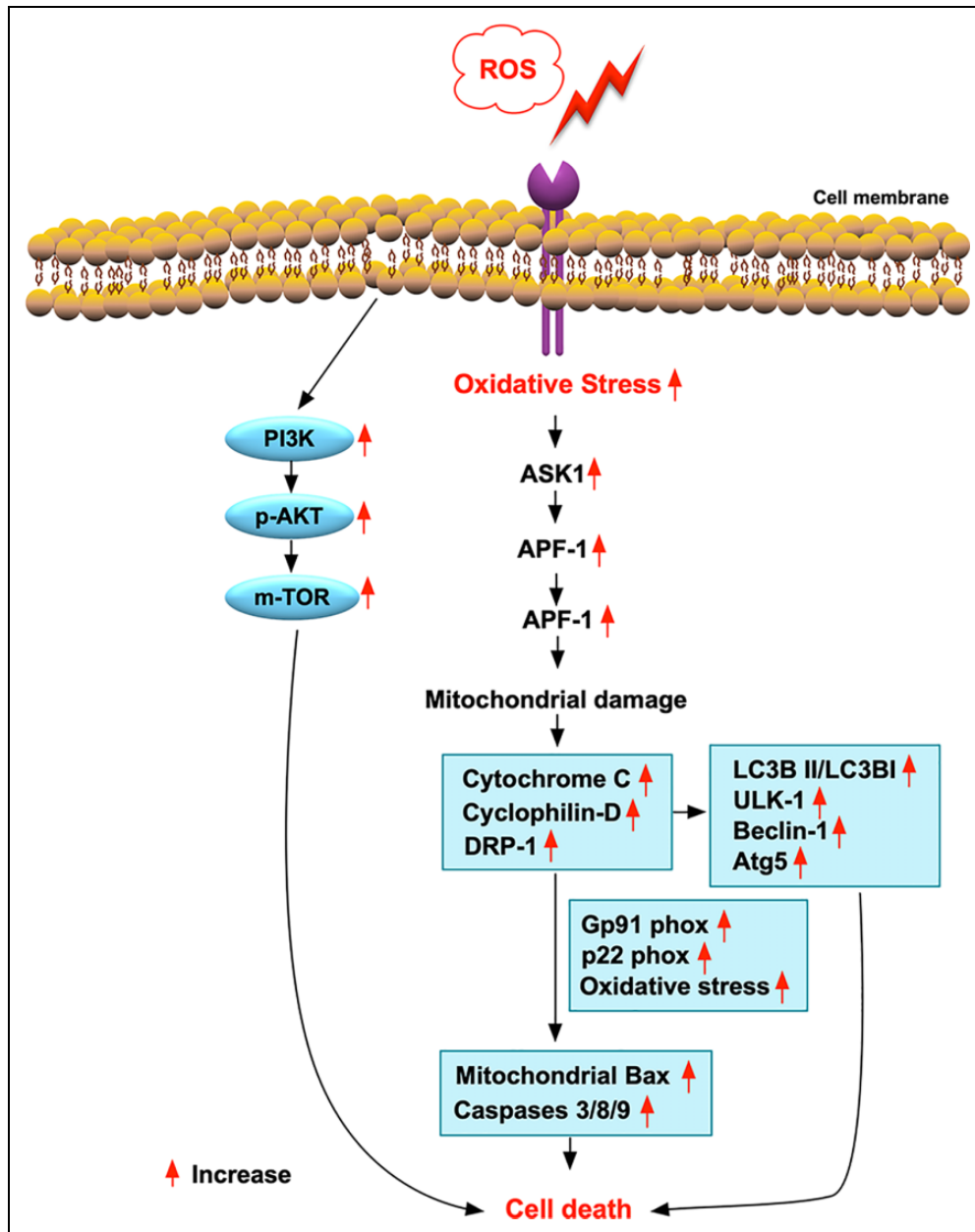


Fig. 5. Schematic proposed mechanism of oxidative stress, cell proliferation/death, mitochondrial, and autophagic signaling pathways in lung epithelial cells undergoing hypoxia–reperfusion stimulation. PI3 K: phosphoinositide 3-kinase; ROS: reactive oxygen species.

identical pattern of inflammatory cells in circulation among the four groups (Fig. 7).

Lung Injury Score, DNA-damaged Biomarker and Inflammatory Infiltration in Lung Parenchyma and Arterial Oxygen Saturation by 72 h After Lung IR Procedure

We further assessed the histopathological findings and cellular levels of the lung parenchymal damage (Figs. 8 and 9). As we expected, the microscopic findings showed that the

lung injury score (i.e., reduced number of alveolar sacs and increased lung crowded score) and the number of γ -H2AX+ cells, an indicator of DNA-damaged biomarker, were lowest in group 1, highest in group 2, and significantly higher in group 3 than in group 4 (Fig. 8). Of interesting findings in the present study were that the patch consolidation and inflammatory infiltrations in lung parenchyma and peribronchial trees were remarkably increased in group 2 than in group 1 that were remarkably suppressed in group 3 and further remarkably suppressed in group 4 (Fig. 8).

On the other hand, the arterial oxygen saturation (%) displayed an opposite pattern of γ -H2AX+ cell expression

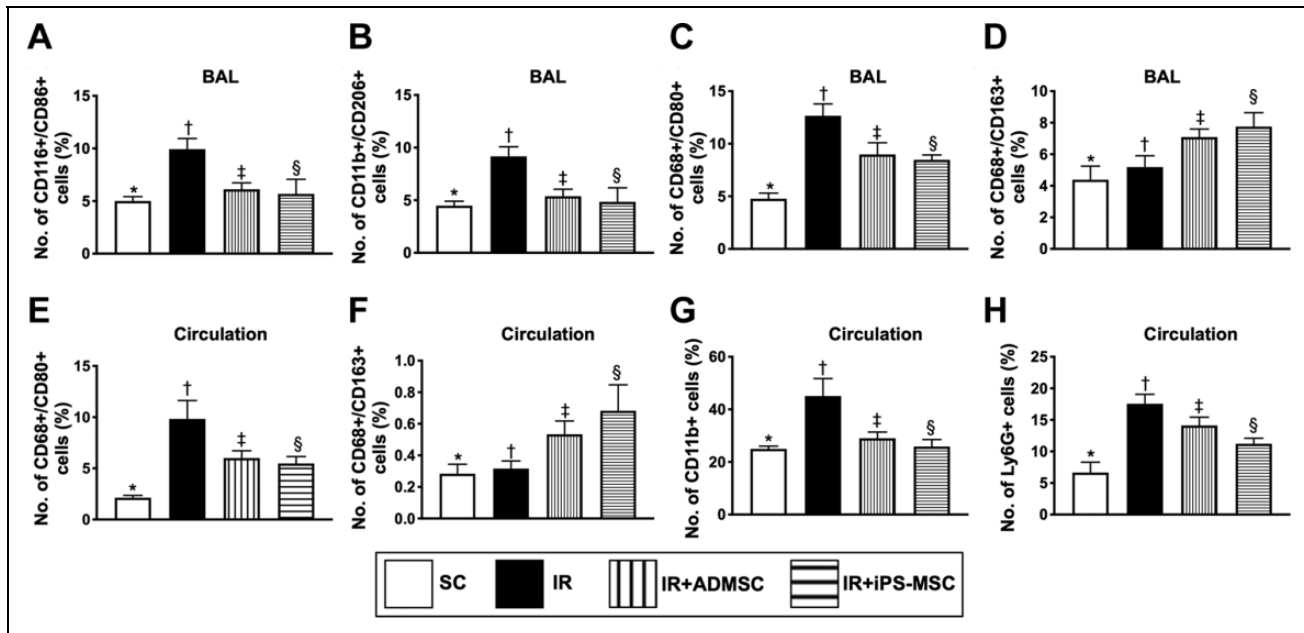


Fig. 6. Flow cytometric analysis of inflammatory cells in BAL fluid and circulation by 72 h after lung IR procedure. (A) Number (%) of CD11b+/CD86+ cells in BAL fluid, * versus other groups with different symbols (†, ‡, §), $P < 0.001$. (B) Number (%) of CD11b+/CD206+ cells in BAL fluid, * versus other groups with different symbols (†, ‡, §), $P < 0.001$. (C) Number (%) of CD68+/CD80+ cells in BAL fluid, * versus other groups with different symbols (†, ‡, §), $P < 0.001$. (D) Number (%) of CD68+/CD163+ cells (i.e., indicates M2-like macrophages) in BAL fluid, * versus other groups with different symbols (†, ‡, §), $P < 0.001$. (E) Number (%) of CD68+/CD80+ cells in circulation, * versus other groups with different symbols (†, ‡, §), $P < 0.001$. (F) Number (%) of CD68+/CD163+ cells in circulation, * versus other groups with different symbols (†, ‡, §), $P < 0.001$. (G) Number (%) of CD11b+ cells in circulation, * versus other groups with different symbols (†, ‡, §), $P < 0.001$. (H) Number (%) of Ly6G+ cells in circulation, * versus other groups with different symbols (†, ‡, §), $P < 0.001$. All statistical analyses were performed by one-way ANOVA, followed by Bonferroni multiple comparison post hoc test ($n = 6$ for each group). Symbols (*, †, ‡, §) indicate significance (at 0.05 level). ADMSCs: adipose tissue-derived mesenchymal stem cells; ANOVA: analysis of variance; BAL: bronchoalveolar lavage; iPS-MSCs: human inducible pluripotent stem cell-derived mesenchymal stem cells; IR: ischemia-reperfusion; SC: sham-operated control.

among the four groups (Fig. 8). Additionally, the protein expressions of F4/80+ and CD14+ cells, two cellular level of inflammation, exhibited an identical pattern of DNA-damaged biomarker among the four groups (Fig. 9).

Protein Expressions of Inflammatory, Mitochondrial-damage/Cell Apoptosis, Autophagic and Oxidative Stress Signaling Pathways in Lung Parenchyma by 72 h After Lung IR Procedure

The protein expressions of TLR4, MyD88, NF- κ B, Cox-2, TNF- α , and IL-1 β , the inflammatory up- and down-stream signalings, were highest in group 2, lowest in group 1, and significantly higher in group 3 than in group 4 (Figs. 10–12). On the other hand, the protein expression of p-IKB α , a protein for transmitting the signaling from the upper to lower signaling pathway, exhibited an opposite pattern of TLR4/MyD88, implying a utilization of p-IKB α was notably required with respect to inflammatory reaction that was ameliorated by MSC therapy (Fig. 10).

Additionally, the protein expressions of cytosolic cytochrome C, DRP1, ASK1, mitochondrial Bax and caspase3,

and index of mitochondrial-damaged/cell apoptotic signaling, revealed an identical pattern of inflammatory signaling among the four groups (Fig. 11). On the other hand, the protein expression of mitochondrial cytochrome C, an indicator of mitochondrial integrity, exhibited an opposite pattern of cytosolic cytochrome C among the four groups.

Furthermore, the protein expressions of ULK1, beclin-1, Atg5 and ratio of LCB3-II/LC3B-I, four indices of autophagy, and protein expressions of gp91phox and p22phox, two indicators of oxidative stress biomarkers, exhibited an identical pattern of apoptosis among the four groups (Fig. 12).

Discussion

This study which investigated the therapeutic impact of ADMSCs and iPS-MSCs on acute lung IRI in rodent yielded several striking implications. First, for the same amount of cell numbers (i.e., 1.2×10^6 cells/at 30 min, 18 h, and 36 h after IR procedure), the xenogeneic iPS-MSCs was not inferior to allogeneic ADMSCs in protecting the rat lung against IRI. Second, the circulatory inflammatory-immune responses were promptly elicited in rodent after acute lung

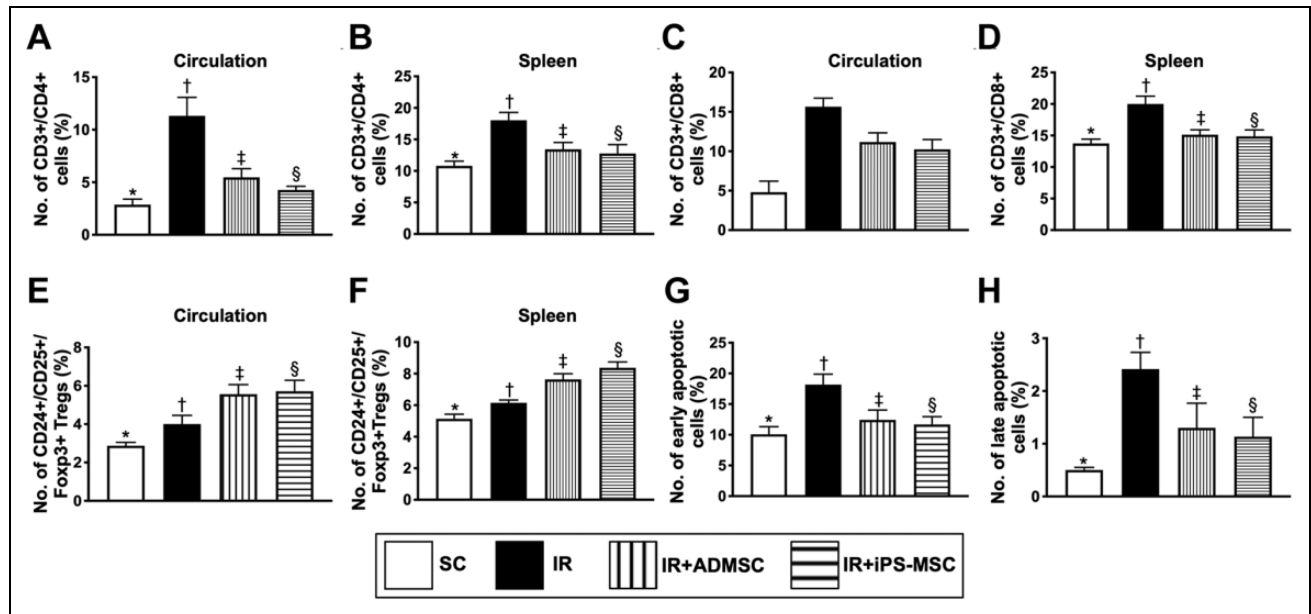


Fig. 7. Flow cytometric analyses of immune and apoptotic cells by 72 h after lung IR procedure. (A) Number (%) of CD3⁺CD4⁺ cells in circulation, * versus other groups with different symbols (†, ‡, §), $P < 0.001$. (B) Number (%) of CD3⁺CD4⁺ cells in spleen, * versus other groups with different symbols (†, ‡, §), $P < 0.001$. (C) Number (%) of CD3⁺CD8⁺ cells in circulation, * versus other groups with different symbols (†, ‡, §), $P < 0.001$. (D) Number (%) of CD3⁺CD8⁺ cells in spleen, * versus other groups with different symbols (†, ‡, §), $P < 0.001$. (E) Number (%) of CD4⁺CD25⁺Foxp3⁺ Tregs in circulation, * versus other groups with different symbols (†, ‡, §), $P < 0.001$. (F) Number (%) of CD4⁺CD25⁺Foxp3⁺ Tregs in spleen, * versus other groups with different symbols (†, ‡, §), $P < 0.001$. (G) Number of early phase (annexin V+/PI-) of apoptotic cells, * versus other groups with different symbols (†, ‡, §), $P < 0.001$. (H) Number of late phase (annexin V+/PI+) apoptotic cells, * versus other groups with different symbols (†, ‡, §), $P < 0.001$. All statistical analyses were performed by one-way ANOVA, followed by Bonferroni multiple comparison post hoc test ($n = 6$ for each group). Symbols (*, †, ‡, §) indicate significance (at 0.05 level). ADMSCs: adipose tissue-derived mesenchymal stem cells; ANOVA: analysis of variance; iPS-MSCs: human inducible pluripotent stem cell-derived mesenchymal stem cells; IR: ischemia-reperfusion; SC: sham-operated control.

IRI. Third, ADMSCs and iPS-MSCs effectively protected the lung from acute IRI mainly through suppressing immune-inflammatory, oxidative stress, mitochondrial-damaged/cell death, and autophagic signaling pathways, highlighting that multiple signaling pathways rather than a single one participated in lung injury after acute IRI development.

The molecular and cellular mechanisms involved in the pathogenesis of ALI/acute lung IRI have been extensively investigated by previous studies^{5,12-16}. Intriguingly, majority of these studies have focused on clarifying one rather than multiple signaling pathways of causing the lung organ damages^{5,12-16,43-46}. An essential finding of the *in vitro* result demonstrated that the inflammatory, oxidative stress, mitochondrial-damaged/cell death, and autophagic signaling pathways were all remarkably upregulated in hypoxia and reperfusion conditions (i.e., mimicked clinical setting of IR injury). These findings implicate that complex rather than a single signaling pathways frequently work together to damage the cells in setting of IRI.

In the *in vitro* study, because the iPS-MSCs were cultured in upper compartment and L2 cells cultured at the bottom of the Transwell, there was no direct contact between iPS-MSCs and L2 cells. However, the inflammatory/oxidative

stress/autophagic signalings were still notably suppressed by iPS-MSCs treatment, suggesting these effects can be attributed to condition medium, i.e., could be the results from the secretions of the paracrine, cytokines, exosomes, etc. from iPS-MSC. Abundant data have previously shown that condition medium and exosomes therapy effectively protected the organs from ischemia-related/IRI^{39,47-50}. In this way, our suggestions are supported by previous studies^{39,47-50}.

An especially interesting new issue should be discussed in the present study was that autophagic signaling was found to be substantially increased on IR lung injury. Intriguingly, our previous studies have also demonstrated that autophagic biomarkers were notably in setting of cardiorenal syndrome⁵¹ and acute ischemic stroke⁵². Other studies have also demonstrated that the autophagy proteins beclin-1, LC3-I, and LC3-II were notably augmented in ALI animals⁵³. Our findings, in addition to being consistent with the results of the previous studies⁵¹⁻⁵³, may raise the need of taken deeply into consideration of this important pathway in ALI, especially when we consider how to offer a safe and effective treatment for the ALI patients.

Our *in vitro* results encourage us to inquire into the *in vivo* condition of a rodent acute lung IRI. As we expected, just

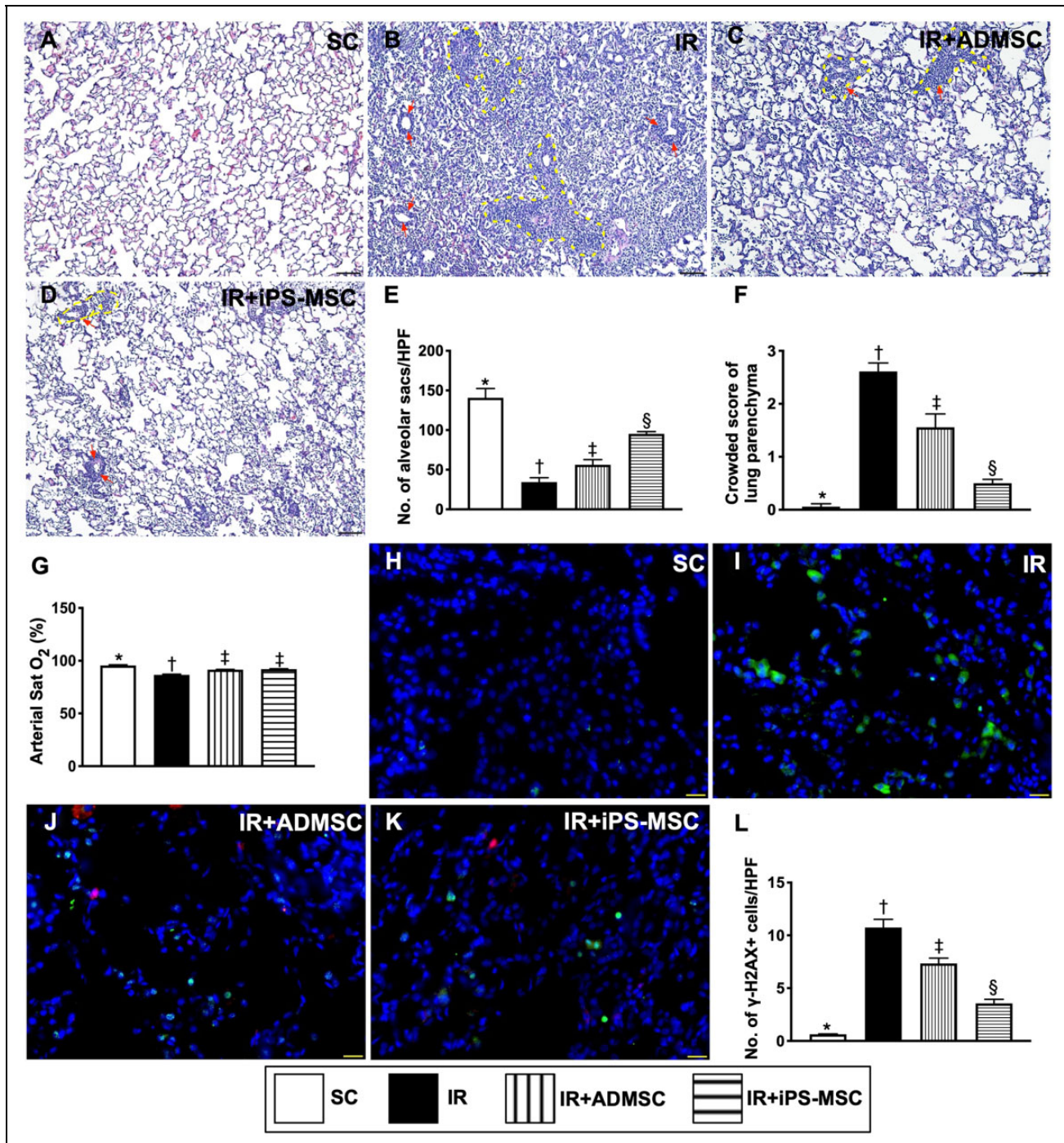


Fig. 8. Histopathological findings in lung parenchyma, arterial oxygen saturation, and DNA-damaged biomarkers at 72 h after lung IR procedure. (A to D) Histopathological findings (i.e., H&E staining) of lung parenchyma under microscopy ($\times 100$) among the four groups. It was worthy notably that abundant inflammatory cell infiltration in the lung parenchyma and peribronchial area (violet color, red arrows), and patch consolidation in lung (yellow dotted lines) were identified to be much higher in IR animals than in other groups of animals. (E) The number of alveolar sacs among four groups, * versus other groups with different symbols (\dagger , \ddagger , \S), $P < 0.0001$. (F) Crowded scores of lung parenchyma, * versus other groups with different symbols (\dagger , \ddagger , \S), $P < 0.0001$. (G) Arterial saturation (Sat) oxygen (O₂) (%), * versus other groups with different symbols (\dagger , \ddagger), $P < 0.001$. (H to K) Illustrating the IF microscopic finding ($\times 400$) for the identification of γ -H2AX+ cells in lung parenchyma (green color). Red color in (J) and (K) indicate the transfused MSCs. (L) Analytical result of number of γ -H2AX+ cells, * versus other groups with different symbols (\dagger , \ddagger , \S), $P < 0.0001$. The scale bars in right lower corner represent 100 μ m. (G) Arterial saturation (Sat) oxygen (O₂) (%), * versus other groups with different symbols (\dagger , \ddagger), $P < 0.001$. The scale bars in right lower corner represent 20 μ m. All statistical analyses were performed by one-way ANOVA, followed by Bonferroni multiple comparison post hoc test ($n = 6$ for each group). Symbols (*, \dagger , \ddagger , \S) indicate significance (at 0.05 level). ADMSCs: adipose tissue-derived mesenchymal stem cells; ANOVA: analysis of variance; H&E: hematoxylin and eosin; HPF: high-power field; IF: immunofluorescent; iPS-MSCs: human inducible pluripotent stem cell-derived mesenchymal stem cells; IR: ischemia-reperfusion; SC: sham-operated control.

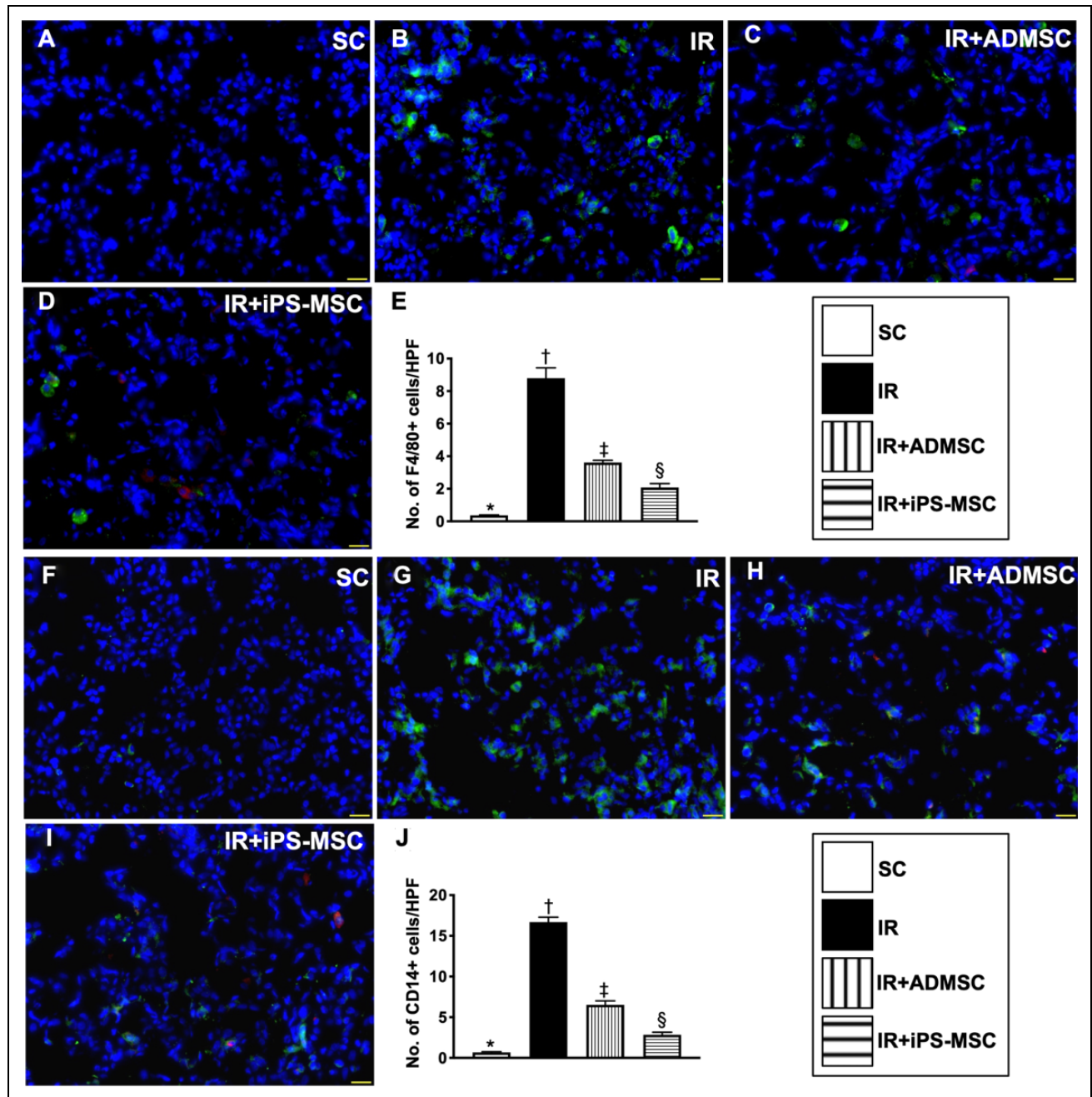


Fig. 9. Inflammatory cell infiltrations in lung parenchyma at 72 h after lung IR procedure. (A to D) Illustrating the IF microscopic finding ($\times 400$) for identification of F4/80+ cells in lung parenchyma (green color). (E) Analytical result of number of F4/80+ cells, * versus other groups with different symbols (\dagger , \ddagger , \S), $P < 0.0001$. (F to I) Illustrating the IF microscopic finding ($\times 400$) for identification of CD14+ cells in lung parenchyma (green color). (J) Analytical result of number of CD14+ cells, * versus other groups with different symbols (\dagger , \ddagger , \S), $P < 0.0001$. Red color in (C), (D), (H), and (I) indicated the transfused MSCs. The scale bars in right lower corner represent 20 μm . All statistical analyses were performed by one-way ANOVA, followed by Bonferroni multiple comparison post hoc test ($n = 6$ for each group). Symbols (*, \dagger , \ddagger , \S) indicate significance (at 0.05 level). ADMSCs: adipose tissue-derived mesenchymal stem cells; ANOVA: analysis of variance; HPF: high-power field; IF: immunofluorescent; iPS-MSCs: human inducible pluripotent stem cell-derived mesenchymal stem cells; IR: ischemia-reperfusion; MSC: mesenchymal stem cell; SC: sham-operated control.

like the *in vitro* results, these inflammatory, oxidative stress, and autophagic downstream signalings were consistently and substantially upregulated in setting of acute lung IRI in rat, highlighting that *in vitro* results strongly supported the findings from the *in vivo* study and implied that these

signaling pathways worked together to damage the lung after acute IRI (refer to Fig. 13).

Lung is a fragile organ susceptible to the damage caused by many different disease entities¹⁻⁸. A principal finding in the present study was that the histological scoring of lung

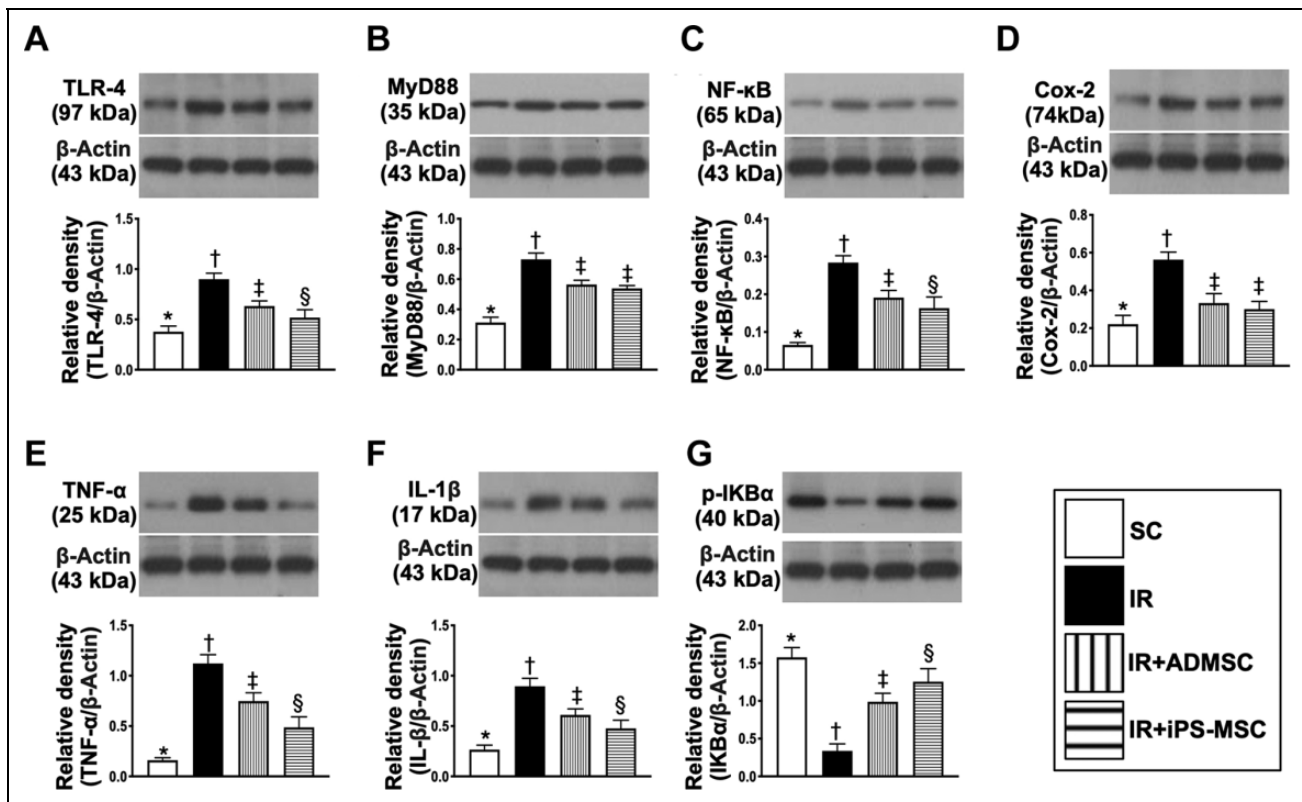


Fig. 10. Protein expression of inflammatory signaling in lung parenchyma at 72 h after lung IR procedure. (A) Protein expressions of TLR4, * versus other groups with different symbols (†, ‡, §), $P < 0.0001$. (B) Protein expression of MyD88, * versus other groups with different symbols (†, ‡), $P < 0.0001$. (C) Protein expression of phosphorylated (p)-NF- κ B, * versus other groups with different symbols (†, ‡, §), $P < 0.0001$. (D) Protein expression of Cox-2, * versus other groups with different symbols (†, ‡), $P < 0.0001$. (E) Protein expression of TNF- α , * versus other groups with different symbols (†, ‡, §), $P < 0.0001$. (F) Protein expression of IL-1 β , * versus other groups with different symbols (†, ‡, §), $P < 0.0001$. (G) Protein expression of p-IKB α , * versus other groups with different symbols (†, ‡, §), $P < 0.0001$. All statistical analyses were performed by one-way ANOVA, followed by Bonferroni multiple comparison post hoc test ($n = 6$ for each group). Symbols (*, †, ‡, §) indicate significance (at 0.05 level). ADMSCs: adipose tissue-derived mesenchymal stem cells; ANOVA: analysis of variance; iPS-MSCs: human inducible pluripotent stem cell-derived mesenchymal stem cells; IR: ischemia-reperfusion; SC: sham-operated control; TNF: tumor necrosis factor.

parenchymal damage (i.e., histopathological finding of lung injury score) was found to markedly increase, whereas the number of alveoli sacs (i.e., sites of gas exchange) was substantially reduced in IR animals as compared to the SC. Accordingly, our findings, in addition to strengthening the findings of previous studies, could explain why the arterial oxygen saturation (i.e., functional status) was notably reduced in the former than the latter group^{1-8,54}. Conclusively, our findings highlighted that acute lung IRI is a complex pathogenetic situation, which involves bronchioalveolar architecture, cellular, and molecular perturbations⁵.

The possible therapeutic strategy to reduce or prevent the acute lung IRI is still largely lacking. The role of ADMSCs and iPS-MSCs on tissue regeneration and organ protection against ischemia/IRI have been individually extensively discussed^{24,26-38}. However, when potency is taken into consideration, there is regrettably lacking works to specifically validate the quality of these two kinds of cells. An intriguing finding in the present study was that, by administrating an

equal amount of cells at exactly the same time points through the identical route to animal, the iPS-MSCs was superior to ADMSCs for downregulating the signaling pathways of inflammation, immune reaction, generations of oxidative stress and autophagy, mitochondrial damage and apoptosis, resulting in a more eminently reduced lung injury score and protecting the lung architecture. In light of this observation, our *in vitro* study supported the *in vivo* findings that transcended those of previous studies^{24,26-38}.

Multiple dosages of antibiotic use are one of the most common methods for successful treatment of infectious diseases in our daily clinical practice. Interestingly, our previous study has also shown that two successive dosages and early treatment were superior to single dosage and delayed treatment for suppressing post-heart transplant acute rejection in rat⁵⁴. Based on the concept of early treatment and the results of our previous study, we administered the allogenic/xenogeneic MSCs to the lung IR animals at the time points of 30 min, 18 h, and 36 h after IR procedure. Even more importantly, our findings are not only safe but also promising⁵⁴.

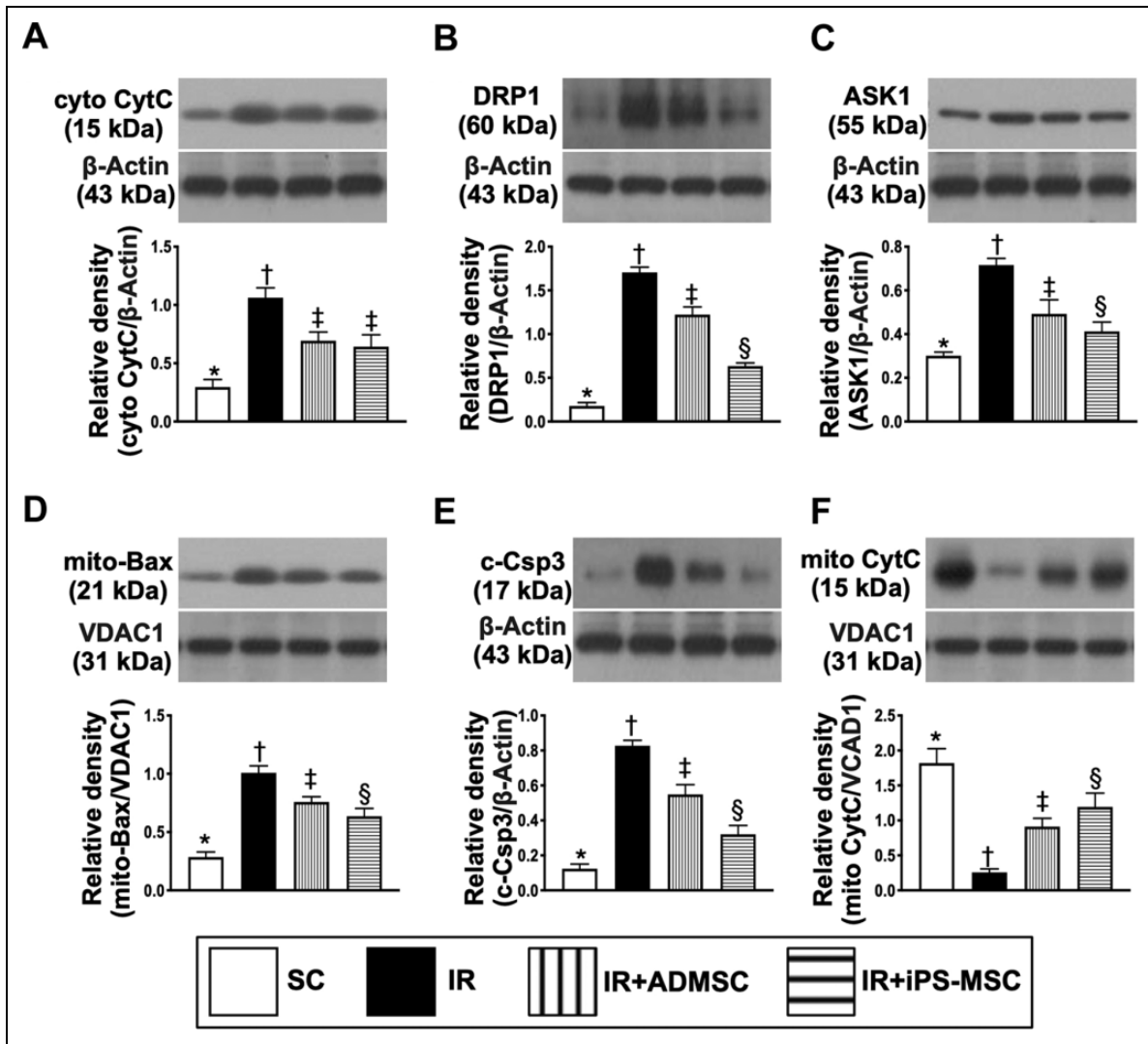


Fig. 11. Protein expressions of mitochondrial-damage/cell apoptosis signaling pathways in lung parenchyma at 72 h after lung IR procedure. (A) Protein expression of cyto-CytC, * versus other groups with different symbols (†, ‡, §), $P < 0.0001$. (B) Protein expression of DRP1, * versus other groups with different symbols (†, ‡, §), $P < 0.0001$. (C) Protein expression of ASK1, * versus other groups with different symbols (†, ‡, §), $P < 0.0001$. (D) Protein expression of mitochondrial (mito)-Bax, * versus other groups with different symbols (†, ‡, §), $P < 0.0001$. (E) Protein expression of c-Csp3, * versus other groups with different symbols (†, ‡, §), $P < 0.0001$. (F) Protein expression of mito-CytC, * versus other groups with different symbols (†, ‡, §), $P < 0.0001$. All statistical analyses were performed by one-way ANOVA, followed by Bonferroni multiple comparison post hoc test ($n = 6$ for each group). Symbols (*, †, ‡, §) indicate significance (at 0.05 level). ADMSCs: adipose tissue-derived mesenchymal stem cells; ANOVA: analysis of variance; ASK1: apoptosis signal-regulating kinase 1; c-Csp3: cleaved caspase 3; cyto-CytC: cytosolic cytochrome C; DRP1: dynamin-related protein 1; iPS-MSCs: human inducible pluripotent stem cell-derived mesenchymal stem cells; IR: ischemia-reperfusion; mito-CytC: mitochondrial cytochrome C; SC: sham-operated control.

Pathophysiological changes and pathological findings of ALI always raise the investigator's interesting. In this study, the inflammatory cell infiltration in the lung parenchyma was clearly identified in IR animals. Additionally, the concentration of albumin in BAL was also found to markedly increase in the IR animals, suggesting a result of exudate leakage due to a pathologically increased the permeability of lung parenchyma. Furthermore, the patch consolidation in the lung parenchyma was clearly observed in the IR animals. These findings along with the findings of lung injury scores in the present study highlight that the rat lung parenchyma

underwent a pulmonary swelling and edema as well as an acute inflammatory reaction. These findings may explain why patients with acute severe lung injury will frequently develop into the setting of acute respiratory distress syndrome⁵⁵.

Study Limitation

This study has limitations. First, although the results were attractive and promising, the study period was relatively short. Accordingly, the long-term outcome of iPS-MSCs/

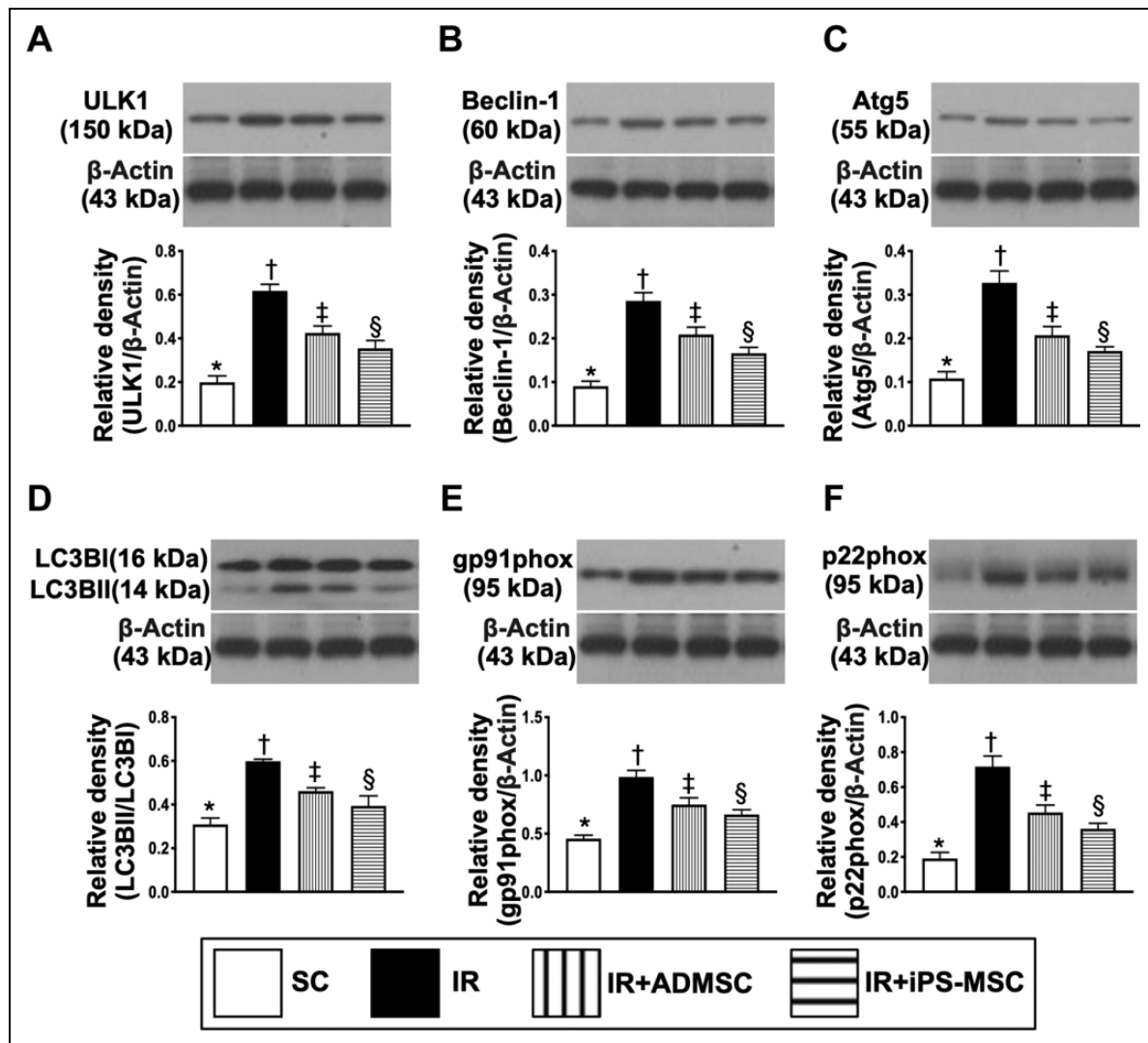


Fig. 12. Protein expressions of autophagic and oxidative stress signaling pathways in lung parenchyma at 72 h after lung IR procedure. (A) Protein expression of ULK1, * versus other groups with different symbols (†, ‡, §), $P < 0.0001$. (B) Protein expression of beclin-1, * versus other groups with different symbols (†, ‡, §), $P < 0.0001$. (C) Protein expression of Atg5, * versus other groups with different symbols (†, ‡, §), $P < 0.0001$. (D) Protein ratio of LC3B-II/LC3B-I, * versus other groups with different symbols (†, ‡, §), $P < 0.0001$. (E) Protein expression of gp91phox, * versus other groups with different symbols (†, ‡, §), $P < 0.0001$. (F) Protein expression of p22phox, * versus other groups with different symbols (†, ‡, §), $P < 0.0001$. All statistical analyses were performed by one-way ANOVA, followed by Bonferroni multiple comparison post hoc test ($n = 6$ for each group). Symbols (*, †, ‡, §) indicate significance (at 0.05 level). ADMSCs: adipose tissue-derived mesenchymal stem cells; ANOVA: analysis of variance; iPS-MSCs: human inducible pluripotent stem cell-derived mesenchymal stem cells; IR: ischemia-reperfusion; SC: sham-operated control.

ADMSCs remained uncertain. Second, this study did not perform the stepwise increased dosage of iPS-MSCs or ADMSCs on treatment of acute lung IR. Therefore, the therapeutic impact of iPS-MSCs on protecting the lung from IR injury was superior to ADMSCs or vice versa remained to be clarified. Third, this study did not assess the physiological changes that occurred in the left lung during the clamping procedure. Additionally, 30 min of ischemia, followed by reperfusion of the rat lung in the present study did not cause acute severe lung injury that might not mimicking the true clinical settings of acute

severe lung IR injury, especially in the procedure of lung transplantation. Accordingly, the effect of ADMSCs and iPS-MSCs shown by this study should be further evaluated for more obviously understanding the therapeutic impact of the cell therapy on severe rat lung IR injury prior to applying the cell-based therapy in our future clinical practice.

In conclusion, iPS-MSCs/ADMSCs protected the lung against IR injury mainly through attenuating the inflammatory/oxidative stress/mitochondrial-damaged/autophagic signaling pathways.

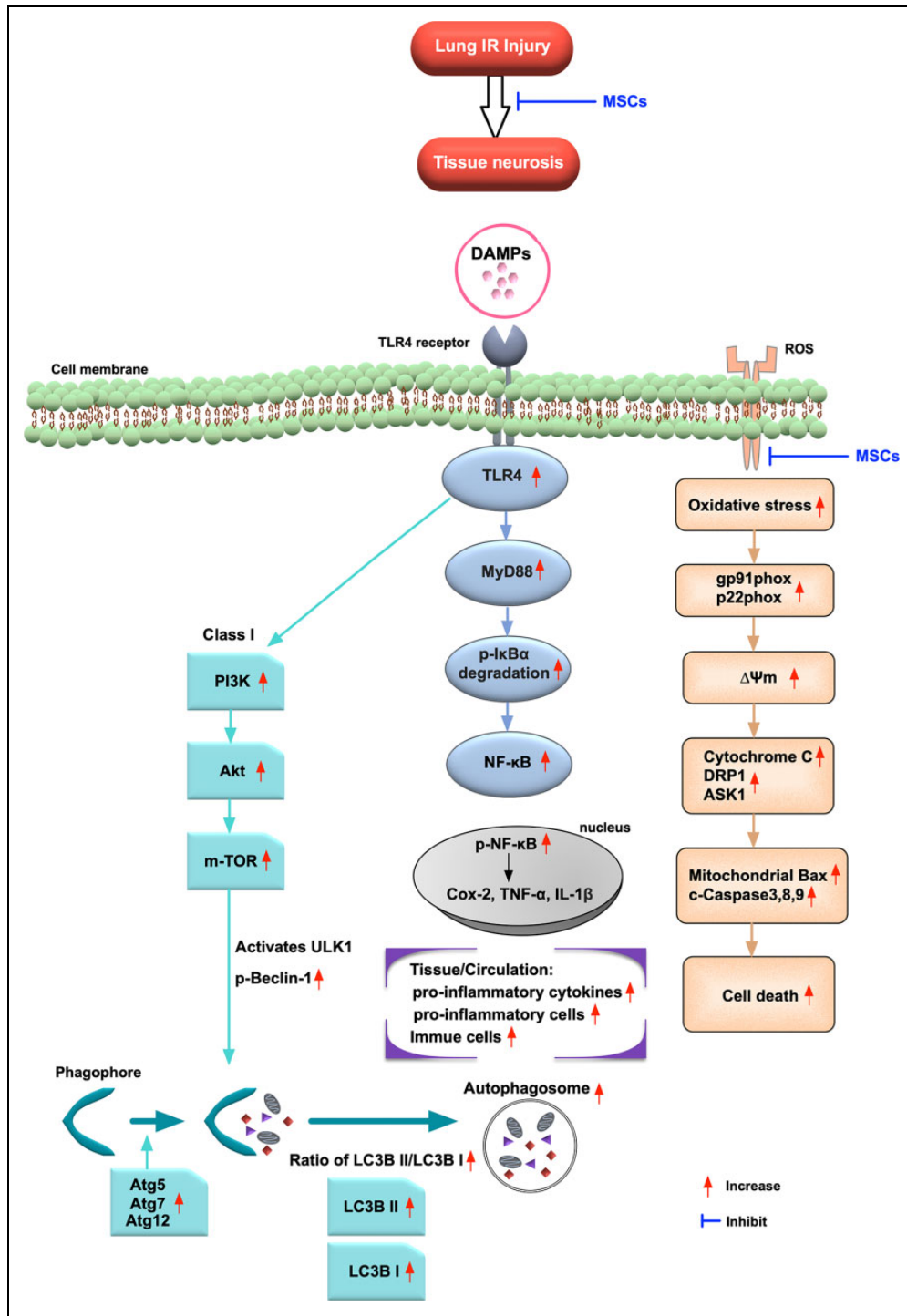


Fig. 13. The schematic proposed mechanism of inflammatory, oxidative stress, mitochondrial-damage/cell death, and autophagic signaling pathways in acute lung IRI based on the findings from an animal model of acute lung IRI. DAMPs: damage-associated molecular patterns; IRI: ischemia-reperfusion injury; MSCs: mesenchymal stem cells; ROS: reactive oxygen species.

Author Contributions

Kun-Chen Lin: funding acquisition and project administration. Jun-Ning Yeh and Yi-Ling Chen: methodology and investigation. John Y. Chiang: writing-review and editing. Pei-Hsun Sung and Fan-Yen Li: data curation and validation. Jun Guo:

writing original. Hon-Kan Yip: writing-original, review and editing.

Ethical Approval

This article does not contain any studies with human.

Statement of Human and Animal Rights

All procedures with patients in this study were conducted in accordance with the Animal Ethics Committee of the Chang Gung Memorial Hospital, Kaohsiung.

Statement of Informed Consent

This article does not contain any studies with human.


Declaration of Conflicting Interests

The authors declared no potential conflicts of interest with respect to the research, authorship, and/or publication of this article.

Funding

The author(s) disclosed receipt of the following financial support for the research, authorship, and/or publication of this article: This study was supported by a program grant from Chang Gung Memorial Hospital, Chang Gung University (Grant number: CMRPG8H0331).

ORCID iD

Hon-Kan Yip  <https://orcid.org/0000-0002-6305-5717>

Supplemental Material

Supplemental material for this article is available online.

References

- Ailawadi G, Lau CL, Smith PW, Swenson BR, Hennessy SA, Kuhn CJ, Fedoruk LM, Kozower BD, Kron IL, Jones DR. Does reperfusion injury still cause significant mortality after lung transplantation? *J Thorac Cardiovasc Surg.* 2009;137(3):688–694.
- Bittner HB, Binner C, Dahlberg P, Mohr FW. Reducing ischemia-reperfusion injury in clinical lung transplantation. *Transplant Proc.* 2007;39(2):489–492.
- Ciesla DJ, Moore EE, Johnson JL, Burch JM, Cothren CC, Sauaia A. The role of the lung in postinjury multiple organ failure. *Surgery.* 2005;138(4):749–757; discussion 757–758.
- Cobelens PM, van Putte BP, Kavelaars A, Heijnen CJ, Kesecioglu J. Inflammatory consequences of lung ischemia-reperfusion injury and low-pressure ventilation. *J Surg Res.* 2009;153(2):295–301.
- den Hengst WA, Gielis JF, Lin JY, Van Schil PE, De Windt LJ, Moens AL. Lung ischemia-reperfusion injury: a molecular and clinical view on a complex pathophysiological process. *Am J Physiol Heart Circ Physiol.* 2010;299(5):H1283–1299.
- Fiser SM, Tribble CG, Long SM, Kaza AK, Kern JA, Jones DR, Robbins MK, Kron IL. Ischemia-reperfusion injury after lung transplantation increases risk of late bronchiolitis obliterans syndrome. *Ann Thorac Surg.* 2002;73(4):1041–1047; discussion 1047–1048.
- Matthay MA, Zimmerman GA. Acute lung injury and the acute respiratory distress syndrome: four decades of inquiry into pathogenesis and rational management. *Am J Respir Cell Mol Biol.* 2005;33(4):319–327.
- Phua J, Badia JR, Adhikari NK, Friedrich JO, Fowler RA, Singh JM, Scales DC, Stather DR, Li A, Jones A, Gattas DJ. Has mortality from acute respiratory distress syndrome decreased over time?: A systematic review. *Am J Respir Crit Care Med.* 2009;179(3):220–227.
- Hashimoto N, Takeyoshi I, Tsutsumi H, Sunose Y, Tokumine M, Totsuka O, Ohwada S, Matsumoto K, Morishita Y. Effects of a bradykinin B(2) receptor antagonist on ischemia-reperfusion injury in a canine lung transplantation model. *J Heart Lung Transplant.* 2004;23(5):606–613.
- McCourtie AS, Farivar AS, Woolley SM, Merry HE, Wolf PS, Mackinnon-Patterson B, Keech JC, Fitzsullivan E, Mulligan MS. Alveolar macrophage secretory products effect type 2 pneumocytes undergoing hypoxia-reoxygenation. *Ann Thorac Surg.* 2008;86(6):1774–1779.
- Wolf PS, Merry HE, Farivar AS, McCourtie AS, Mulligan MS. Stress-activated protein kinase inhibition to ameliorate lung ischemia reperfusion injury. *J Thorac Cardiovasc Surg.* 2008;135(3):656–665.
- Garcia-Covarrubias L, Manning EW, 3rd, Sorell LT, Pham SM, Majetschak M. Ubiquitin enhances the Th2 cytokine response and attenuates ischemia-reperfusion injury in the lung. *Crit Care Med.* 2008;36(3):979–982.
- Geudens N, Wuyts WA, Rega FR, Vanaudenaerde BM, Neyrinck AP, Verleden GM, Lerut TE, Van Raemdonck DE. N-acetyl cysteine attenuates the inflammatory response in warm ischemic pig lungs. *J Surg Res.* 2008;146(2):177–183.
- Iwata T, Chiyo M, Yoshida S, Smith GN Jr, Mickler EA, Presson R Jr, Fisher AJ, Brand DD, Cummings OW, Wilkes DS. Lung transplant ischemia reperfusion injury: metalloprotease inhibition down-regulates exposure of type V collagen, growth-related oncogene-induced neutrophil chemotaxis, and tumor necrosis factor-alpha expression. *Transplantation.* 2008;85(3):417–426.
- Ovechkin AV, Lominadze D, Sedoris KC, Robinson TW, Tyagi SC, Roberts AM. Lung ischemia-reperfusion injury: implications of oxidative stress and platelet-arteriolar wall interactions. *Arch Physiol Biochem.* 2007;113(1):1–12.
- Seekamp A, Mulligan MS, Till GO, Smith CW, Miyasaka M, Tamatani T, Todd RF 3rd, Ward PA. Role of beta 2 integrins and ICAM-1 in lung injury following ischemia-reperfusion of rat hind limbs. *Am J Pathol.* 1993;143(2):464–472.
- An Y, Liu WJ, Xue P, Ma Y, Zhang LQ, Zhu B, Qi M, Li LY, Zhang YJ, Wang QT, Jin Y. Autophagy promotes MSC-mediated vascularization in cutaneous wound healing via regulation of VEGF secretion. *Cell Death Dis.* 2018;9(2):58.
- Chen C, Chen W, Li Y, Dong Y, Teng X, Nong Z, Pan X, Lv L, Gao Y, Wu G. Hyperbaric oxygen protects against myocardial reperfusion injury via the inhibition of inflammation and the modulation of autophagy. *Oncotarget.* 2017;8(67):111522–111534.
- Dang S, Yu ZM, Zhang CY, Zheng J, Li KL, Wu Y, Qian LL, Yang ZY, Li XR, Zhang Y, Wang RX. Autophagy promotes apoptosis of mesenchymal stem cells under inflammatory microenvironment. *Stem Cell Res Ther.* 2015;6:247.
- Liu L, Jin X, Hu CF, Li R, Zhou Z, Shen CX. Exosomes derived from mesenchymal stem cells rescue myocardial ischaemia/reperfusion injury by inducing cardiomyocyte

- autophagy via AMPK and Akt pathways. *Cell Physiol Biochem*. 2017;43(1):52–68.
21. Sung PH, Lee FY, Lin LC, Chen KH, Lin HS, Shao PL, Li YC, Chen YL, Lin KC, Yuen CM, Chang HW, et al. Melatonin attenuated brain death tissue extract-induced cardiac damage by suppressing DAMP signaling. *Oncotarget*. 2018;9(3):3531–3548.
 22. Tong WW, Zhang C, Hong T, Liu DH, Wang C, Li J, He XK, Xu WD. Silibinin alleviates inflammation and induces apoptosis in human rheumatoid arthritis fibroblast-like synoviocytes and has a therapeutic effect on arthritis in rats. *Sci Rep*. 2018;8(1):3241.
 23. Kadri SS, Miller AC, Hohmann S, Bonne S, Nielsen C, Wells C, Gruver C, Quraishi SA, Sun J, Cai R, Morris PE, et al. Risk factors for in-hospital mortality in smoke inhalation-associated acute lung injury: data from 68 united states hospitals. *Chest*. 2016;150(6):1260–1268.
 24. Komiya K, Akaba T, Kozaki Y, Kadota JI, Rubin BK. A systematic review of diagnostic methods to differentiate acute lung injury/acute respiratory distress syndrome from cardiogenic pulmonary edema. *Crit Care*. 2017;21(1):228.
 25. Schmickl CN, Biehl M, Wilson GA, Gajic O. Comparison of hospital mortality and long-term survival in patients with acute lung injury/ARDS vs cardiogenic pulmonary edema. *Chest*. 2015;147(3):618–625.
 26. Chang CL, Sung PH, Sun CK, Chen CH, Chiang HJ, Huang TH, Chen YL, Zhen YY, Chai HT, Chung SY, Tong MS, et al. Protective effect of melatonin-supported adipose-derived mesenchymal stem cells against small bowel ischemia-reperfusion injury in rat. *J Pineal Res*. 2015;59(2):206–220.
 27. Chen HH, Lin KC, Wallace CG, Chen YT, Yang CC, Leu S, Chen YC, Sun CK, Tsai TH, Chen YL, Chung SY, et al. Additional benefit of combined therapy with melatonin and apoptotic adipose-derived mesenchymal stem cell against sepsis-induced kidney injury. *J Pineal Res*. 2014;57(1):16–32.
 28. Chen YT, Chiang HJ, Chen CH, Sung PH, Lee FY, Tsai TH, Chang CL, Chen HH, Sun CK, Leu S, Chang HW, et al. Melatonin treatment further improves adipose-derived mesenchymal stem cell therapy for acute interstitial cystitis in rat. *J Pineal Res*. 2014;57(3):248–261.
 29. Le Blanc K, Tammik L, Sundberg B, Haynesworth SE, Ringden O. Mesenchymal stem cells inhibit and stimulate mixed lymphocyte cultures and mitogenic responses independently of the major histocompatibility complex. *Scand J Immunol*. 2003;57(1):11–20.
 30. Maumus M, Guerit D, Toupet K, Jorgensen C, Noel D. Mesenchymal stem cell-based therapies in regenerative medicine: applications in rheumatology. *Stem Cell Res Ther*. 2011;2(2):14.
 31. Thum T, Bauersachs J, Poole-Wilson PA, Volk HD, Anker SD. The dying stem cell hypothesis: immune modulation as a novel mechanism for progenitor cell therapy in cardiac muscle. *J Am Coll Cardiol*. 2005;46(10):1799–1802.
 32. Chau M, Deveau TC, Song M, Wei ZZ, Gu X, Yu SP, Wei L. Transplantation of iPSC cell-derived neural progenitors overexpressing SDF-1alpha increases regeneration and functional recovery after ischemic stroke. *Oncotarget*. 2017;8(57):97537–97553.
 33. Jung JH, Fu X, Yang PC. Exosomes generated from iPSC-derivatives: new direction for stem cell therapy in human heart diseases. *Circ Res*. 2017;120(2):407–417.
 34. Lee PY, Chien Y, Chiou GY, Lin CH, Chiou CH, Tarng DC. Induced pluripotent stem cells without c-Myc attenuate acute kidney injury via downregulating the signaling of oxidative stress and inflammation in ischemia-reperfusion rats. *Cell Transplant*. 2012;21(12):2569–2585.
 35. Tachibana A, Santoso MR, Mahmoudi M, Shukla P, Wang L, Bennett M, Goldstone AB, Wang M, Fukushi M, Ebert AD, Woo J, et al. Paracrine effects of the pluripotent stem cell-derived cardiac myocytes salvage the injured myocardium. *Circ Res*. 2017;121(6):e22–e36.
 36. Toyohara T, Mae S, Sueta S, Inoue T, Yamagishi Y, Kawamoto T, Kasahara T, Hoshina A, Toyoda T, Tanaka H, Araoka T, et al. Cell therapy using human induced pluripotent stem cell-derived renal progenitors ameliorates acute kidney injury in mice. *Stem Cells Transl Med*. 2015;4(9):980–992.
 37. Wang Y, Zhang L, Li Y, Chen L, Wang X, Guo W, Zhang X, Qin G, He SH, Zimmerman A, Liu Y, et al. Exosomes/microvesicles from induced pluripotent stem cells deliver cardioprotective miRNAs and prevent cardiomyocyte apoptosis in the ischemic myocardium. *Int J Cardiol*. 2015;192:61–69.
 38. Yoshida Y, Yamanaka S. Induced pluripotent stem cells 10 years later: for cardiac applications. *Circ Res*. 2017;120(12):1958–1968.
 39. Sun CK, Chen CH, Chang CL, Chiang HJ, Sung PH, Chen KH, Chen YL, Chen SY, Kao GS, Chang HW, Lee MS, et al. Melatonin treatment enhances therapeutic effects of exosomes against acute liver ischemia-reperfusion injury. *Am J Transl Res*. 2017;9(4):1543–1560.
 40. Sun CK, Yen CH, Lin YC, Tsai TH, Chang LT, Kao YH, Chua S, Fu M, Ko SF, Leu S, Yip HK. Autologous transplantation of adipose-derived mesenchymal stem cells markedly reduced acute ischemia-reperfusion lung injury in a rodent model. *J Transl Med*. 2011;9:118.
 41. Ko SF, Chen YT, Wallace CG, Chen KH, Sung PH, Cheng BC, Huang TH, Chen YL, Li YC, Chang HW, Lee MS, et al. Inducible pluripotent stem cell-derived mesenchymal stem cell therapy effectively protected kidney from acute ischemia-reperfusion injury. *Am J Transl Res*. 2018;10(10):3053–3067.
 42. Chang CL, Leu S, Sung HC, Zhen YY, Cho CL, Chen A, Tsai TH, Chung SY, Chai HT, Sun CK, Yen CH, et al. Impact of apoptotic adipose-derived mesenchymal stem cells on attenuating organ damage and reducing mortality in rat sepsis syndrome induced by cecal puncture and ligation. *J Transl Med*. 2012;10:244.
 43. de Perrot M, Liu M, Waddell TK, Keshavjee S. Ischemia-reperfusion-induced lung injury. *Am J Respir Crit Care Med*. 2003;167(4):490–511.
 44. Fisher AB, Dodia C, Tan ZT, Ayene I, Eckenhoff RG. Oxygen-dependent lipid peroxidation during lung ischemia. *J Clin Invest*. 1991;88(2):674–679.

45. Ishiyama T, Dharmarajan S, Hayama M, Moriya H, Grapperhaus K, Patterson GA. Inhibition of nuclear factor kappaB by IkappaB superrepressor gene transfer ameliorates ischemia-reperfusion injury after experimental lung transplantation. *J Thorac Cardiovasc Surg.* 2005;130(1):194–201.
46. Kaminski A, Pohl CB, Sponholz C, Ma N, Stamm C, Vollmar B, Steinhoff G. Up-regulation of endothelial nitric oxide synthase inhibits pulmonary leukocyte migration following lung ischemia-reperfusion in mice. *Am J Pathol.* 2004;164(6):2241–2249.
47. Chen KH, Chen CH, Wallace CG, Yuen CM, Kao GS, Chen YL, Shao PL, Chen YL, Chai HT, Lin KC, Liu CF, et al. Intravenous administration of xenogenic adipose-derived mesenchymal stem cells (ADMSC) and ADMSC-derived exosomes markedly reduced brain infarct volume and preserved neurological function in rat after acute ischemic stroke. *Oncotarget.* 2016;7(46):74537–74556.
48. Leu S, Kao YH, Sun CK, Lin YC, Tsai TH, Chang LT, Chua S, Yeh KH, Wu CJ, Fu M, Yip HK. Myocardium-derived conditioned medium improves left ventricular function in rodent acute myocardial infarction. *J Transl Med.* 2011;9:11.
49. Lin KC, Yip HK, Shao PL, Wu SC, Chen KH, Chen YT, Yang CC, Sun CK, Kao GS, Chen SY, Chai HT, et al. Combination of adipose-derived mesenchymal stem cells (ADMSC) and ADMSC-derived exosomes for protecting kidney from acute ischemia-reperfusion injury. *Int J Cardiol.* 2016;216:173–185.
50. Ophelders DR, Wolfs TG, Jellema RK, Zwanenburg A, Andriessen P, Delhaas T, Ludwig AK, Radtke S, Peters V, Janssen L, Giebel B, et al. Mesenchymal stromal cell-derived extracellular vesicles protect the fetal brain after hypoxia-ischemia. *Stem Cells Transl Med.* 2016;5(6):754–763.
51. Yang CC, Chen YT, Wallace CG, Chen KH, Cheng BC, Sung PH, Li YC, Ko SF, Chang HW, Yip HK. Early administration of empagliflozin preserved heart function in cardiorenal syndrome in rat. *Biomed Pharmacother.* 2019;109:658–670.
52. Lin KC, Chen KH, Wallace CG, Chen YL, Ko SF, Lee MS, Yip HK. Combined therapy with hyperbaric oxygen and melatonin effectively reduce brain infarct volume and preserve neurological function after acute ischemic infarct in rat. *J Neuropathol Exp Neurol.* 2019;78(10):949–960.
53. Zhang X, Zheng J, Yan Y, Ruan Z, Su Y, Wang J, Huang H, Zhang Y, Wang W, Gao J, Chi Y, et al. Angiotensin-converting enzyme 2 regulates autophagy in acute lung injury through AMPK/mTOR signaling. *Arch Biochem Biophys.* 2019;672:108061.
54. Yip HK, Lee MS, Sun CK, Chen KH, Chai HT, Sung PH, Lin KC, Ko SF, Yuen CM, Liu CF, Shao PL, et al. Therapeutic effects of adipose-derived mesenchymal stem cells against brain death-induced remote organ damage and post-heart transplant acute rejection. *Oncotarget.* 2017;8(65):108692–108711.
55. Yip HK, Fang WF, Li YC, Lee FY, Lee CH, Pei SN, Ma MC, Chen KH, Sung PH, Lee MS. Human umbilical cord-derived mesenchymal stem cells for acute respiratory distress syndrome. *Crit Care Med.* 2020;48(5):e391–e399.